

AD-A225 682

2  
DTIC FILE COPY

CONTRACT NO:

DAMD17-88-C-8148

TITLE:

Characterization of the *P. brevis* Polyether Neurotoxin Binding  
Component in Excitable Membranes

PRINCIPAL INVESTIGATOR:

Daniel G. Baden

PI ADDRESS:

University of Miami  
Rosenstiel School of Marine and Atmospheric Science  
Division of Marine Biology and Fisheries  
4600 Rickenbacker Causeway  
Miami Florida 33149

REPORT DATE:

1 June 1990

TYPE OF REPORT:

Midterm

PREPARED FOR:

U.S. ARMY MEDICAL RESEARCH AND DEVELOPMENT COMMAND  
FORT DETRICK  
FREDERICK MARYLAND 21702-5012

DISTRIBUTION STATEMENT:

Approved for public release;  
distribution unlimited

DTIC  
S ELECTE D  
AUG 23 1990  
Co D

90 00 20 0411

## REPORT DOCUMENTATION PAGE

Form Approved  
OMB No. 0704-0188

1a. REPORT SECURITY CLASSIFICATION Unclassified			1b. RESTRICTIVE MARKINGS		
2a. SECURITY CLASSIFICATION AUTHORITY			3. DISTRIBUTION / AVAILABILITY OF REPORT Approved for public release; distribution unlimited		
2b. DECLASSIFICATION / DOWNGRADING SCHEDULE					
4. PERFORMING ORGANIZATION REPORT NUMBER(S)			5. MONITORING ORGANIZATION REPORT NUMBER(S)		
6a. NAME OF PERFORMING ORGANIZATION University of Miami		6b. OFFICE SYMBOL (If applicable)	7a. NAME OF MONITORING ORGANIZATION		
6c. ADDRESS (City, State, and ZIP Code) Rosenstiel School of Marine and Atmospheric Science Miami, Florida 33149-1098			7b. ADDRESS (City, State, and ZIP Code)		
8a. NAME OF FUNDING / SPONSORING ORGANIZATION U.S. Army Medi- cal Research and Development		8b. OFFICE SYMBOL (If applicable)	9. PROCUREMENT INSTRUMENT IDENTIFICATION NUMBER DAMD17-88-C-8148		
8c. ADDRESS (City, State, and ZIP Code) Fort Detrick, Frederick, MD 21702-5012			10. SOURCE OF FUNDING NUMBERS		
			PROGRAM ELEMENT NO. 0602787A	PROJECT NO. 3M1- 62787A871	TASK NO. AA
			WORK UNIT ACCESSION NO. 388		
11. TITLE (Include Security Classification) (U) Characterization of the <u>P. brevis</u> Polyether Neuro- toxin Binding Component in Excitable Membranes					
12. PERSONAL AUTHOR(S) Daniel G. Baden					
13a. TYPE OF REPORT Midterm		13b. TIME COVERED FROM 8/15/88 TO 2/14/90		14. DATE OF REPORT (Year, Month, Day) 1990 June 1	
15. PAGE COUNT 31					
16. SUPPLEMENTARY NOTATION					
17. COSATI CODES			18. SUBJECT TERMS (Continue on reverse if necessary and identify by block number)		
FIELD	GROUP	SUB-GROUP	marine toxins, sodium channel, photoaffinity probe affinity column, receptor binding, brevetoxin, saxitoxin, tetrodotoxin, veratridine. RA 1-65		
06	20				
06	15				
19. ABSTRACT (Continue on reverse if necessary and identify by block number) The development of a functional model, and topographic picture of how and why sodium channels act in the ways in which they gate sodium ion flux is our goal. We are developing about 20 different natural toxin derivatives based on 7 divergent chemical modifications. Each type of derivative has a specific potential once synthesized. Photoaffinity probes, affinity columns, tritiated non-exchangeable toxins, and specific intermediates are in various stages of completion. These probes are being utilized to characterize the topographic relationship of sites 1, 2, and 5 associated with voltage-sensitive sodium channels. The brevetoxin binding site has already been localized on Domain IV of VSSC, and binds to an external hydrophobic peptide located between S5 and S6 of Domain IV. Antisodium channel RIA, tritiated brevetoxin photoaffinity binding, immunoprecipitation, and SDS-polyacrylamide gel electrophoresis have all made substantial contributions to brevetoxin site localization.					
20. DISTRIBUTION / AVAILABILITY OF ABSTRACT <input type="checkbox"/> UNCLASSIFIED/UNLIMITED <input checked="" type="checkbox"/> SAME AS RPT. <input type="checkbox"/> DTIC USERS			21. ABSTRACT SECURITY CLASSIFICATION Unclassified		
22a. NAME OF RESPONSIBLE INDIVIDUAL Mary Frances Bostian			22b. TELEPHONE (Include Area Code) 301-663-7325		22c. OFFICE SYMBOL SGRD-RMI-S

## FOREWORD

Opinions, interpretations, conclusions and recommendations are those of the author and are not necessarily endorsed by the US Army.

\_\_\_\_\_ Where copyrighted material is quoted, permission has been obtained to use such material.


\_\_\_\_\_ Where material from documents designated for limited distribution is quoted, permission has been obtained to use the material.

X Citations of commercial organizations and trade names in this report do not constitute an official Department of the Army endorsement or approval of the products or services of these organizations.

X In conducting research using animals, the investigators adhered to the "Guide for the Care and Use of Laboratory Animals of the Institute of Laboratory Resources, National Research Council (NIH Publication No. 86-23, Revised 1985).

\_\_\_\_\_ For the protection of human subjects, the investigators adhered to policies of applicable Federal Law 45 CFR 46.

\_\_\_\_\_ In conducting research utilizing recombinant DNA technology, the investigators adhered to current guidelines promulgated by the National Institutes of Health.

 6/19/90  
\_\_\_\_\_  
PI-Signature Date

Accession For	
NTIS	CRA&I <input checked="" type="checkbox"/>
DTIC	TAB <input type="checkbox"/>
Unannounced	<input type="checkbox"/>
Justification	
By _____	
Distribution /	
Availability Codes	
Dist	Avail and/or Special
A-1	



## TABLE OF CONTENTS

LIST OF TABLES AND FIGURES	2
INTRODUCTION	4
<u>Nature of the problem</u>	4
<u>Background</u>	5
<u>Purpose of Present Work</u>	7
<i>Photoaffinity Probes</i>	7
<i>Affinity Columns</i>	7
<i>Radioactive Toxins</i>	8
<i>Enzyme-Synthesized Tritiated Brevetoxins</i>	8
BODY	8
<u>Experimental Methods</u>	8
<i>Photoaffinity Probes</i>	8
<i>Brevetoxin Affinity Columns</i>	12
<i>Tetrodotoxin Modifications</i>	12
<i>Saxitoxin Derivatives</i>	15
<i>Brevetoxin Binding Site</i>	17
<u>Results</u>	19
<i>Brevetoxin Binding Site Characterization</i>	19
<i>Optimizing Brevetoxin Photoaffinity Probe Covalent Modification of Sodium Channels</i>	20
<i>Optimizing Brevetoxin Photoaffinity Probe Binding</i>	22
<i>Saxitoxin Derivatives</i>	28
<i>Tetrodotoxin Derivatives</i>	28
<i>Brevetoxin Derivatives</i>	28
<i>Photoaffinity Probes</i>	28
CONCLUSIONS	28
REFERENCES	30

## LIST OF TABLES AND FIGURES

### TABLES

Table 1.	Receptor Binding Sites Associated with VSSC	4
----------	---	---

### FIGURES

Figure 1.	Subunit structure of sodium channel	5
Figure 2.	Catterall's functional map of the $\alpha$ -subunit of voltage-sensitive sodium channel	6
Figure 3.	Schematic representation of the "sliding" helix S4 region of voltage-sensitive sodium channel	6
Figure 4.	Organic scheme for producing a radioiodinatable photoaffinity probe with multifunctional capability	8
Figure 5.	Compound I, 3- <i>p</i> -azidophenyl 2- <i>p</i> -hydroxyphenyl propionic acid	8
Figure 6.	Compound II, 3- <i>p</i> -azidophenyl 2- <i>p</i> -hydroxyphenyl propionic acid ethylene diamine monoamide	9
Figure 7.	Compound III, 2- <i>p</i> -tetrahydropyranyloxyphenyl, 3- <i>p</i> -azidophenyl propionic acid	10
Figure 8.	Compound IV. Brevetoxin photoaffinity probe	11
Figure 9.	Compound V. <i>p</i> -azidobenzoic acid	11
Figure 10.	Compound VI. Brevetoxin <i>p</i> -azidobenzoic acid	11
Figure 11.	Brevetoxin aminobexyl Sepharose	12
Figure 12.	Tetrodotoxin, illustrating C-11 and C-6 functionalities to be exploited in derivatives	12
Figure 13.	Protecting groups for primary alcohol on tetrodotoxin	13
Figure 14.	Dimethoxytrityl tetrodotoxin	13
Figure 15.	Dimethoxytrityl-benzylated tetrodotoxin (a), and deprotected benzyl tetrodotoxin (b)	14
Figure 16.	Tritiated tetrodotoxin arising from re-reduction of aldehydetetrodotoxin	14
Figure 17.	Anhydroepitetrodotoxin and amino hexyl tetrodotoxin amide	15
Figure 18.	Saxitoxin	15
Figure 19.	Progression for STX organic manipulations	15
Figure 20.	Decarbamoyl saxitoxin	16

Figure 21.	Partial schematic for saxitoxin synthesis	16
Figure 22.	Rosenthal analysis of tritiated PbTx-3-photoaffinity probe to rat brain synaptosomes	19
Figure 23.	Rosenthal analysis of tritiated PbTx-3-photoaffinity probe to rat brain synaptosomes pre-incubated with 5 nM unlabeled toxin-photoaffinity probe	19
Figure 24.	SDS-PAGE analysis of synaptosomes binding to [ $^3\text{H}$ ]PbTx-3 photoprobe on a 5-17.5% gradient gel (panel a), or 5% gels (panel b)	20
Figure 25.	Sephacryl S-300 gel filtration of brevetoxin receptor under non-reducing conditions.	21
Figure 26.	Molecular radius determination of brevetoxin receptor.	22
Figure 27.	Stokes radius calculation	22
Figure 28 & 29	Gel Filtration of modified brevetoxin receptor	23
Figure 30.	DEAE-Sephadex A-25 chromatography	24
Figure 31.	Wheat germ allutinin chromatography	24
Figure 32.	Brevetoxin receptor trypsinization	25
Figure 33.	SDS-PAGE analysis of a NaTPHO treated with 10 $\mu\text{g}/\text{mL}$ TPCK-trypsin	25
Figure 34.	SDS-PAGE analysis of NaTPHO treated with 100 $\mu\text{g}/\text{mL}$ TPCK-trypsin	26
Figure 35.	SDS-PAGE comparison of $^{32}\text{P}$ -labeled and brevetoxin photoaffinity labeled $\alpha$ -subunit of sodium channel	26
Figure 36.	Trypsinization time course and immunoprecipitation using antibodies directed against peptides of the four sodium channel domains	27
Figure 37.	Confirmation of domain IV using anti-SP13 antibodies	27

## INTRODUCTION

### Nature of the Problem

There are seven known sites associated with the voltage-sensitive sodium channel (VSSC) that bind low molecular weight natural toxins with high avidity and affinity (Table 1) [1-9]. The unique nature of each of the binding sites was ascertained using radioactive toxin of one type, and attempting to "compete" away labeled toxin using an excess of unlabeled toxic material. Site 1 is known to bind saxitoxin, tetrodotoxin, and  $\alpha$ -conotoxin, and occupancy at this site blocks passage of sodium ions [10]. Specific binding studies have been carried out using tritium-labeled saxitoxin and  $^{125}$ I-labeled  $\alpha$ -conotoxin. Site 2 exhibits an affinity for batrachotoxin, the grayanotoxins, and the vertrum alkaloids. Binding at this site causes persistent activation of channels. Specific binding studies have used tritiated batrachotoxin  $\alpha$ -benzoate. Site 3 binds sea anemone toxin and the  $\alpha$ -scorpion toxin (*Leiurus quinquestratis*) and enhances persistent activation while inhibiting inactivation. Site 4 binds the  $\beta$ -scorpion toxins (*Centroides suffusus suffusus*), causing repetitive firing and shifting activation voltages. Site 5 binds the trans-fused polyether dinoflagellate brevetoxins and ciguatoxin. Binding at site 5 leads to a shift in activation potential to more negative values, leading to persistent activation at normal membrane potential. Ciguatoxin is the only toxin that has been shown to inhibit the binding of tritiated brevetoxin to site 5. Based on inhibition constant data for ciguatoxin, it must bind with higher affinity than do the brevetoxins. Sites 6 and 7 bind the pyrethroids and pumiliotoxin B; site 6 being allosterically-linked to the brevetoxin site [8,9,11] and site 7 also is linked to site 5 allosterically [12].

TABLE 1. RECEPTOR BINDING SITES ASSOCIATED WITH VSSC <sup>1</sup>

Receptor Site	Ligand	Physiological Effect
1	Tetrodotoxin, saxitoxin, $\alpha$ -conotoxins	Inhibit ion conductance
2	Batrachotoxin, veratrum alkaloids, grayanotoxins	Persistent activation
3	$\alpha$ -Scorpion toxin, sea anemone toxin	Inhibit inactivation
4	$\beta$ -Scorpion toxin	Shift activation
5	Brevetoxins, ciguatoxin	Shift activation, inhibit inactivation
6	Pyrethroids	Shift activation, inhibit inactivation
7	Pumiliotoxin B	Inhibit inactivation

<sup>1</sup> from reference [13].

Highly specific ligands like the natural toxins, have been indispensable in the description of the topographic and functional character of the VSSC. These specific ligands have aided in determination of sodium channel number, in localization of sodium channels in tissues, in developing working hypotheses on the allosteric functional properties of the channel, in identification and purification of individual protein components which make up the channels, and in development of new therapeutics which mimic the action of these drugs [14].

These tasks can be successfully undertaken for several reasons: (i) most of the natural toxins are available in purified forms and sufficient quantities for micro-organic manipulation; (ii) each toxin type interacts with their channel binding site with affinities in the nM to pM concentration ranges; (iii) toxin structures may be manipulated to provide derivatives which aid in developing structure-activity relationships; (iv) toxin structure may be modified in conservative ways which produce radioactive, photoaffinity-linked, and solid-support

immobilized derivatives. For purposes of this research, we have chosen to direct our attention to the production and study of ligand derivatives specific for VSSC sites 1, 2, and 5—those defined sites for which the ligands are non-proteinaceous natural toxins.

These toxin probes shall be utilized to study the interaction with Site 1 (saxitoxin and derivatives, tetrodotoxin), site 2 (batrachotoxin, veratridine, aconitine, and the grayanotoxins), or site 5 (brevetoxins) on sodium channels.

The following derivatives have been, or shall be, synthesized:

- (a) solid-support linked brevetoxin, batrachotoxin, veratridine, and saxitoxin columns;
- (b) photoaffinity-linked derivatives of tritium-labeled brevetoxins;
- (c) non-toxic brevetoxin photoaffinity derivatives;
- (d) tritium-labeled tetrodotoxin and saxitoxin, batrachotoxin, and veratridine and their corresponding photoaffinity labels;
- (e) high specific activity  $^{125}$ Iodine-labeled photoaffinity-coupled saxitoxin, batrachotoxin, veratridine, and brevetoxin;
- (f) enzyme-synthesized brevetoxin (PbTx-3) with theoretical specific activities approaching 50 Ci/mmol; and
- (g)  $^{14}$ Carbon brevetoxin (PbTx-3).

The derivatives are being, or shall be, utilized to:

- (a) determine the spatial relationship of Site 1, Site 2, and Site 5 in rat brain synaptosomes;
- (b) isolate and purify Site 1, Site 2, and Site 5 toxin binding components from rat brain synaptosomes;
- (c) characterize specific binding receptors in other model systems like neuroblastoma cell lines;
- (d) investigate the characteristics of brevetoxin receptors in pulmonary cell lines;
- (e) investigate brevetoxin metabolism in an hepatocyte tissue culture model system.

### Background

Sodium channels isolated from rat brain consist of three separate and separable protein subunits, the  $\alpha$ -subunit and  $\beta_1$ - and  $\beta_2$ -subunits, a 1:1:1 stoichiometry composing the channel [15]. The  $\alpha$ -subunit is a glycoprotein of approximately 260 kDa molecular weight is a transmembrane protein which binds neurotoxins at specific positions on its topographic surface. The two  $\beta$ -subunits are smaller molecular weight peptides (ca. 30 kDa each) and are integral membrane subunit glycoproteins. A schematic representation of the voltage-sensitive sodium channel is given in figure 1.

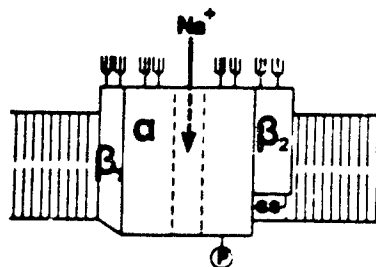


Figure 1. Subunit structure of sodium channel. Disulfide bonds are indicated by (S-S), phosphorylation sites by (P), and glycosylation sites by pitchforks. Removal of the  $\beta_1$ -subunit causes loss of specific saxitoxin binding [14], and solubilization reduces specific binding at sites 2 and 3 [16]. The primary structure of the  $\alpha$ -subunit has been determined [17] and the subunit has been cloned [18]. Diagram is from ref. [15]



Using the primary structure data [17,18], Catterall [15] developed a model for how the  $\alpha$ -subunit inserts itself into the membrane of excitable cell types. Each  $\alpha$ -subunit consists of 4 homologous domains; each homologous domain being composed of 6 transmembrane peptide sequences (figure 2). Using site-directed antibodies, Catterall has shown that specific sites are phosphorylated during activation and inactivation, and using  $^{125}$ I-labeled  $\alpha$ -scorpion toxin in conjunction with protein A-sepharose precipitation of antibody-toxin associations [15]. Within each domain, the 6 transmembrane sequences also appear to be conserved [17], with the highly positively charged S4 regions (denoted by "+" in the figure) being most highly conserved [18]. These S4 domains have been postulated to completely transverse the membrane, and all 4 S4 regions in concert contribute to the ion shuttling ability of the  $\alpha$ -subunit [15].

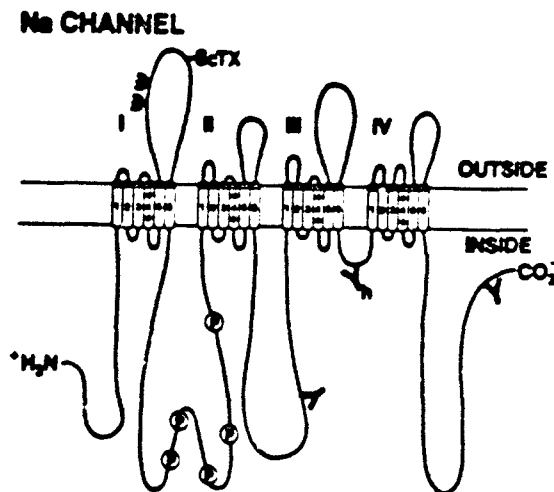


Figure 2. Catterall's functional map of the  $\alpha$ -subunit of voltage-sensitive sodium channel. The  $\alpha$ -subunit of sodium channel (modified from [8]) is shown with phosphorylation sites, with sites of specific interaction with antibodies, glycosylation sites, and scorpion toxin binding site. The S4 region, shown with "+" charge is thought to be responsible for voltage-sensitive ion transport, perhaps by the "sliding helix" model [15].

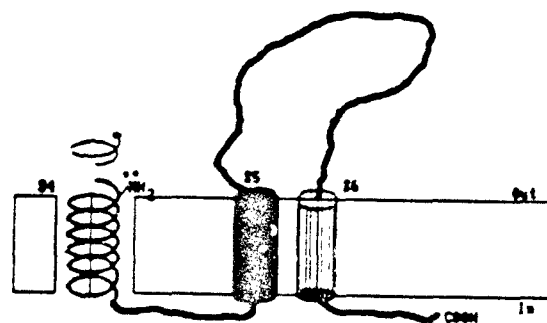


Figure 3. Schematic representation of the "sliding helix" S4 region of voltage-sensitive sodium channel. In response to changes on membrane potential, the 4-S4 regions of  $\alpha$ -subunit of sodium channel rotate, sequentially revealing and burying epsilon-amino groups of lysine along the helical S4 domains. Acting in concert, the 4 individual S4 regions in domains I-IV act to induce a net charge movement which could account for net  $\text{Na}^+$  transport across membranes by ion pairing or charge repulsion.

### Purpose of the Present Work

The development of a functional model, and a topographic picture of how and why  $\alpha$ -subunit acts in the way in which it does, is central to the goals of this contract work. Once functional maps have been developed, the molecular mechanism and mechanics of VSSC action can be explained. The work we are undertaking involves the development and use of no fewer than 20 different natural toxin derivatives based on 7 divergent chemical modifications. Each type of derivative has a specific potential use once synthesized. The chemical methods by which each toxin type is derivatized is different, but the "probes" developed are similar.

**Photoaffinity Probes.** As already described briefly in the Introduction, and amply reported in the literature, physiological and pharmacological aspects of toxin interaction with VSSC are well documented. The critical element of photoaffinity probes is their ability to form covalent attachments with the specific receptors associated with the pharmacological action. The inherent usefulness of radioactive photoaffinity probes is that the label does not dissociate under conditions of receptor denaturation, making it possible to experimentally purify the receptor and utilize the radioactivity as a specific marker for the receptor. At the molecular level, peptides to which natural toxin ligands attach can be identified by SDS polyacrylamide gel electrophoresis, if the labeled toxin is attached covalently and is "hot" enough radiochemically. Molecular weights can be determined, and specific enzymatic cleavage of photoaffinity linked materials can be undertaken. Ultimately, a purified low molecular weight peptide can be sequenced to determine the precise amino acid to which the toxin binds.

A second useful technique is to use specific anti-sodium channel antibodies to detect peptide which contain labeled photoaffinity probes attached. Or, anti-toxin antibodies can be used in Western blots of polyacrylamide gels to ascertain peptides which have unlabeled toxin photoprobes attached. Additional photoaffinity labeled toxins can be utilized to ascertain the identical or different nature of peptides which bind two types of toxins. Similarly, if both low and high affinity sites are postulated, competitive toxin ligands can be used to displace photoaffinity probes from high or low affinity sites, thereby labeling only one of two or more receptor sub-types. Certainly, several different photoaffinity linked toxin probes would be useful in determining polypeptide distance relationships, multiplicity, and allostery.

Isolation of larger quantities of specific toxin receptor requires some type of non-dissociable label, and photoaffinity probes satisfy this requirement exquisitely. Since the label in the bulk solution is rapidly inactivated, the observed specificity should be greater than that obtained with toxin alone under the same conditions. This means that label activated in the bulk solution cannot contribute to the site-specific labeling. If the nitrenes generated react as rapidly with adjacent solvent molecules as expected, labeling should be highly specific, even with excess label. Thus, photoaffinity labeling of low, as well as high, affinity sites should be possible. Also, labeling of hydrophobic sites should be possible, since nitrene produced upon photolysis can react with carbon-hydrogen bonds as well as nucleophilic functions.

For different uses, we shall describe the synthesis of two different types of photoaffinity probe. The first is of small size (relative to the toxins themselves) and is tritiated in a non-exchangeable form. The second is a more elaborate probe, employable for carboxylic acid, amine, and hydroxyl linkage, and is iodlatable. The latter type will be most applicable to autoradiography and rapid non-quantitative measurement. The former will likely more specifically probe the high affinity binding sites in close proximity to the active sites of receptors.

**Affinity Columns.** In theory, affinity chromatography offers the most straightforward means of purifying natural toxin binding sites because it relies on well-defined biospecific binding properties of receptors to accomplish purification. With specific toxin-receptors dissociation constants in the nM to pM concentration ranges, time constants for purification range from several minutes to a couple of days. Problems which arise during affinity chromatography can include such diverse encounters as: (i) receptor being irreversibly bound due to very high affinity (fortunately not a usual case); (ii) loss of receptor activity upon solubilization prior to affinity separation; (iii) the low percentage of sought receptor in the entire milieu of material applied to the column leading to "masking" of ligand on the column; and (iv) coupled ligand which loses its ability to reversibly bind receptor.

Regardless, affinity chromatography is a useful technique, especially if something is known about the active site on the ligand (and one succeeds in coupling to the solid support in another area of the molecule), and if the receptor can be removed from the membrane bound matrix is a somewhat intact (receptor-wise) form. This latter requirement may be met by co-chromatography with other membrane constituents, in lipid vesicles, or in native bilayer environments. Site 2 loses its activity in solubilized form, and so we expect to utilize constituent co-chromatography. Site 1 loses its activity if one of the  $\alpha$ -subunits is removed, and so constituent peptide chromatography will be employed in this case. By all accounts, site 5 maintains its binding integrity in soluble form, and so is probably the most easily approached purification.

**Radioactive Toxins.** This particular area is probably the most difficult to approach for several reasons: (i) the toxins produced in radioactive form should be as close to the original toxin structure as possible. This generally involve oxidation and reduction reactions to introduce tritium into the molecules; (ii) the tritium introduced should be non-exchangeable. This is to say, the tritium should not exchange for hydrogen with either solvent or any biological material. Many tritiated toxins presently available suffer from back-exchange reactions; (iii) the tritium introduced should be of high specific activity, preferably 20-100 Ci/mole. Only three companies make isotopes for labeling at this specific activity, and the availability is limited and difficult to schedule; (iv) the labeled toxin should be stable in aqueous solution for binding studies.

For metabolic studies, brevetoxins should be available in a uniformly labeled form, and of  $^{14}\text{C}$  composition. We anticipate making this material in cultures using radioactive bicarbonate and fixing carbon dioxide for toxin synthesis.

**Enzyme Synthesized Tritiated Brevetoxins.** Based on our past knowledge about the metabolic interconversion of brevetoxin PbTx-2 (aldehyde) to brevetoxin PbTx-3 (alcohol), catalyzed by alcohol dehydrogenase, we anticipate being able to tritiate brevetoxins by an  $\text{NAD}^3\text{H}$  reaction using yeast alcohol dehydrogenase. The expected specific activity being very high relative to chemical reductions, and specific. Oxidation of PbTx-2 to the carboxylic acid followed by enzymatic reduction will yield a toxin in which two tritiums are added per molecule, thereby doubling the specific activity. Reduction of PbTx-3 to PbTx-9 (reduction of the  $\alpha$ -methylene) would add another two tritiums if done in tritiated solvent, leading to a toxin with a conservative specific activity of 50 Ci/mole.

## BODY

### Experimental Methods

**Photoaffinity Probes.** Synthesis of Radioiodinatable Photoaffinity Probes (Figure 4).

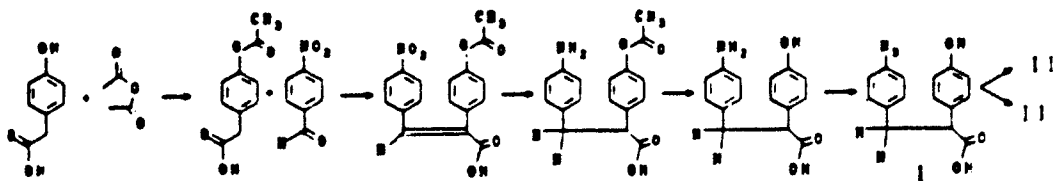


Figure 4. Organic scheme for producing a radioiodinatable photoaffinity probe with multifunctional capability.

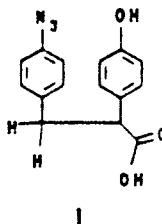


Figure 5. Compound 1, 3-p-azidophenyl 2-p-hydroxyphenyl propionic acid.

**Synthesis of I:** [*p*-acetoxypheylacetic acid]. *p*-Hydroxyphenyl acetic acid (100 g) was dissolved in 72 mL acetic anhydride. The reaction was initiated by the addition of 2-3 drops concentrated sulfuric acid and was stirred. Upon cooling, the acetate separated. The acetate precipitate was redissolved in ether, washed 4 times with water, and was dried over  $\text{Na}_2\text{SO}_4$ . The solution was filtered and flash-evaporated, and the residue dried over phosphorus pentoxide *in vacuo* (yield 105 g, 82.5%).

[2-*p*-acetoxyphenyl *p*-nitro cinnamic acid] [19]. To 100 g *p*-acetoxyphenylacetic acid was added 100 g *p*-nitrobenzaldehyde, 182 mL acetic anhydride, and 91 mL triethylamine and the solution was refluxed for 2.5 hr. The resulting dark liquid was poured with stirring onto an ice-water mixture acidified with sulfuric acid. An oil separated, and solidified in 0.5 hr at 4°C. The solid was filtered by suction, washed thoroughly with ice water, and was recrystallized from 500 mL boiling glacial acetic acid containing 10 mL acetic anhydride. By precipitation with water, and recrystallization from 100 mL glacial acetic acid, a second yield of crystalline product was obtained (yield 145.5 g of yellow crystals, 67.8% mp 146°C).

[3-*p*-aminophenyl 2-*p*-hydroxyphenyl propionic acid hydrochloride]. Fifty grams of the preceding intermediate was hydrogenated in tetrahydrofuran solution in a Parr hydrogenator with 10% Palladium-charcoal, gently heating to prevent clogging of the gas inlet tube. After the theoretical amount of hydrogen was consumed, the warm solution was filtered and the filtrate was flash-evaporated. The residue was refluxed for 1.25 hr in 700 mL 1:1 aqueous HCl solution. After partial cooling, the solution was filtered on fluted filter paper and the filtrate was allowed to crystallize at 4°C. The product was filtered on a glass membrane filter and dried *in vacuo* over KOH (yield 36 g, 81.1%, mp 215°C).

[3-*p*-azidophenyl 2-*p*-hydroxyphenyl propionic acid] [20]. Thirty-seven grams (0.125 mole) of amine hydrochloride intermediate was dissolved in a mixture of 25.8 mL sulfuric acid and 143 mL water. On cooling, a suspension results. Aqueous sodium nitrite (11.92 g in 109 mL water) was added dropwise to the cold stirred suspension, which resulted in full solubilization. Excess nitrous acid was decomposed by the addition of solid urea. The solution was treated with Norite and was filtered by suction. Sodium azide (15.6 g in 80.3 mL water) was added dropwise to the cold stirred solution, and the azidophenyl compound precipitated. After 1 hr at 4°C on ice, the product was filtered by suction and was washed with cold water and dried *in vacuo* over KOH. The dried product (I) was recrystallized from 115 mL boiling glacial acetic acid, washed with cold glacial acetic acid, and was dried *in vacuo* over KOH (yield 27.8 g, 78.6%, mp 182°C).

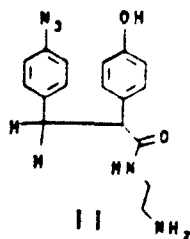
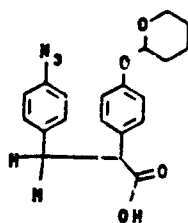


Figure 6. Compound II, 3-*p*-azidophenyl 2-*p*-hydroxyphenyl propionic acid ethylene diamine monoamide.

**Synthesis of II:** [2-*p*-hydroxyphenyl 3-*p*-azidophenyl propionyl ethylene diamine monoamide]. 27.4 g of (I) and 22 g *p*-nitrophenol were dissolved in 40 mL dimethylformamide<sup>4</sup>. Dicyclohexyl carbodiimide (16.2 g in 10 mL dimethylformamide) was added to the stirred solution dropwise, and stirring was continued for 2 more hr on ice. With stirring, the solution was allowed to equilibrate to room temperature and after 1 hr, 10 mL glacial acetic acid was added and the suspension was stirred 15 min longer. The urea was removed by filtration, and was washed with 35 mL tetrahydrofuran. The combined filtrates were poured onto ice and immediately a total volume of 600 mL oil separated. The oil was decanted and extracted with benzene; the benzene layer was washed four times with 10% NaCl solution, and was dried over sodium sulfate. A solution composed of 20 mL ethylene diamine and 100 mL benzene was cooled on ice, and the dried oil extract was added dropwise under vigorous stirring over a period of two hr. A yellow precipitate was filtered by suction, the solid was suspended in a minimum volume of 10% v/v sulfuric acid, and was extracted repeatedly with ethyl acetate to remove *p*-nitrophenol from the yellow gummy layer. The dark aqueous layer formed crystals upon standing at 4°C. The product is the sulfate salt of (II) (yield based on (I) is 51.6%, mp 145°C). This salt is poorly soluble in water compared to the hydrochloride. Preparation of the free base can be accomplished by adding a saturated sodium carbonate solution to a stirred aqueous suspension of the sulfate salt until the solution becomes alkaline. The free base precipitated and after drying was recrystallized from hot ethanol (mp 196°C).



111

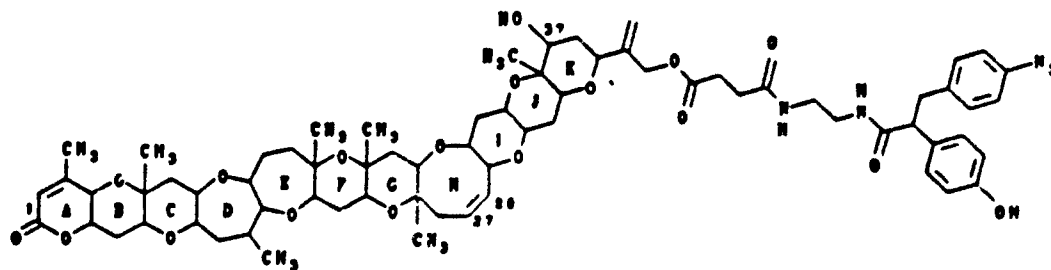
Figure 7. Compound III. 2-*p*-tetrahydropyranyloxyphenyl, 3-*p*-azidophenyl propionic acid.

**Synthesis of III:** [2-*p*-tetrahydropyranyloxyphenyl, 3-*p*-azidophenyl propionic acid]. 3.4 g (I) was suspended in 10 mL dihydropyran and stirred with a glass rod moistened with *p*-toluene sulfonic acid. Mixture produced an exothermic reaction, resulting in a single phase. One hr later, 10 mL of 2M alcoholic KOH was added and the solution was heated in a water bath at 60°C for two hr. The solution was flash-evaporated and 200 mL 5% potassium sulfate solution was added. The solution was mixed with 400 mL ethyl acetate and the mixture was cooled to 0°C. To this solution was added 10 mL cold concentrated sulfuric acid, and the mixture was shaken. The ethyl acetate layer was washed three times with ice-water to pH neutrality, and was dried by the addition of solid sodium sulfate. The dried solution was flash-evaporated and the residue was redissolved in 40 mL acetone, and applied to preparative silica gel thin-layer chromatography plates. Following chromatography using cyclohexane:ethyl acetate (75:25) as mobile phase, the product was identified ( $R_f = 0.1$ ) and was eluted from the silica gel with acetone. Exposure of eluted compound (III) to 6M HCl in acetone for three hr at room temperature resulted in conversion to I, thus confirming identity of the derivative.

**Coupling to Sodium Channel Activator Brevetoxin:** Voltage-sensitive sodium channels are responsible for the membrane potential-dependent sodium ion gating involved in nerve conduction. One group of marine natural product known as the brevetoxins, biosynthesized by the Florida red tide dinoflagellate *Pyrodinium brevis*, binds to Site 5 associated with the  $\alpha$ -subunit of the channel, inducing an open channel state at normal resting membrane potential<sup>5</sup>. CAUTION: Brevetoxins are potent neurotoxins and should be handled only by persons familiar with proper precautions for handling and treatment, should exposure occur [6]. Photoaffinity-linked brevetoxin PbTx-3 probe was synthesized to ascertain the specific binding site for brevetoxins in the channel. Studies carried out using brevetoxin photoaffinity probes indicate a 1:1 stoichiometry with  $\alpha$ -subunit, a competitive ability to displace radioactive brevetoxin from its specific binding site, and a concentration-dependent increase in specific binding.

Brevetoxin PbTx-2 (5.0 mg) was dried over  $P_2O_5$  and 0.147 mL of a 0.4M cerium chloride solution in methanol was added to the toxin under constant stirring<sup>6</sup>. An equal volume of methanol was added, followed by slow addition of 17.1  $\mu$ L of 0.01 M  $NaBH_4$  solution in dimethyl formamide. This procedure was repeated every 20 minutes until the PbTx-2 was completely reduced, as adjudged by thin-layer chromatography. During the reduction procedure, the suspension of PbTx-2 cleared as product PbTx-3 was formed. The product volume was diluted with water to twice volume, products were extracted with diethyl ether, dried and subjected to reverse phase hplc (C-18 column, 85% isocratic methanol, 215 nm ultraviolet detection), resulting in crystalline PbTx-3 (4.294 mg, 87.4% yield). Proton nmr spectra were obtained on a Varian VXR-300 spectrometer, using  $CDCl_3$  (99.96% enriched) and using TMS as internal standard. Reduction of PbTx-2 resulted in the loss of an aldehyde signal at 9.55 ppm and the shift of the  $\alpha$ -methylene signals from 6.09 ppm (trans) and 6.36 ppm (cis) to 4.94 and 5.11 ppm, respectively. Purified PbTx-3 was dissolved in 0.4 mL redistilled pyridine, and a ten-fold molar excess of succinic anhydride in pyridine was added with stirring. The reaction vial was sealed, and the solution was heated to 85°C for two hr with stirring. The reaction vessel was opened and the solvent dried under a stream of nitrogen. Products were redissolved in methanol and chromatographed on silica gel tlc plates using ethyl acetate/light petroleum (70/30) as mobile phase. Previous experiments using tritiated brevetoxin PbTx-3 indicated that the desired conjugate migrated with an  $R_f$  of 0.25, and tested positive with bromocresol green indicator spray reagent.

PbTx-3-succinate was dissolved in 1 mL pyridine, mixed with two-fold molar excess of dicyclohexylcarbodiimide in 0.5 mL pyridine, and solid equimolar (II). The mixture was sealed in a screw-capped tube and was heated for 2 hr at 85°C in a Nujol bath. Following reaction, the bath was cooled, the pyridine evaporated under vacuum, redissolved in methanol and subjected to silica gel tlc using ethyl acetate/light petroleum (80/20) as mobile phase. The complete PbTx-3-linked 2-*p*-hydroxyphenyl 3-*p*-azidophenyl propionyl ethylene diamine monoamide (IV) was visualized on the plate with iodine vapor, was scraped and eluted with methanol. Probe was stable for 6 months at -20°C in methanol solution.



IV

Figure 8. Compound IV. Brevetoxin protoaffinity probe.

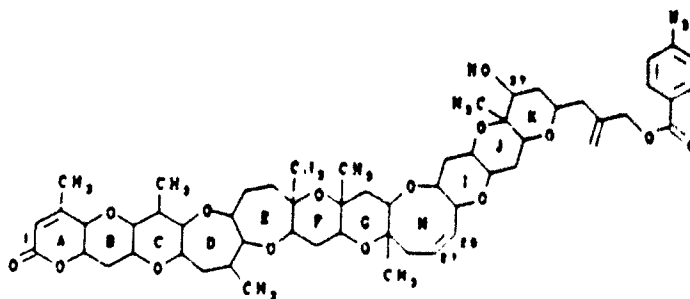


V

Figure 9. Compound V. *p*-azidobenzoic acid.

**Synthesis of V:** [*p*-azidobenzoic acid]. The hydrochloride of *p*-aminobenzoic acid (20 g) was mixed with a solution of 25% HCl (26 mL) in water (100 mL) and was diazotized with a solution of sodium nitrite (9.0 g in 24 mL water) at 0°C. Enough solid urea was added after 20 minutes to destroy the excess nitrous acid, and a solution of sodium azide (9.2 g in 25 mL water) was added dropwise. The precipitated triazobenzoic acid was filtered after 1 hour on an ice bath (yield 22 g, 87%). *p*-azidobenzoic acid recrystallizes from aqueous alcohol in prismatic needles (m.p. 180-181).

The synthesis has been miniaturized, using microglassware, dividing amounts and volumes by 20,000. This yields reagent amount of PABA of 1 mg, and volumes approaching 1-10  $\mu$ L. This miniaturization was required for synthesis of tritiated *p*-azidobenzoic acid. The hydrochloride of *p*-aminobenzoic acid (specific activity of 56 Ci/mmol, ring tritium of nominal position, non-exchangeable) was used in substitution for unlabeled PABA. All other reagents and volumes were reduced in accordance with the tritiated PABA concentration. Following diazotization, instead of filtration we used microcentrifugation to separate solid precipitate from solution, washing once with water to yield tritiated *p*-azidobenzoic acid at 56 Ci/mmol (yield approximately 82% based on tritium recovered).



VI

Figure 10. Compound VI. Brevetoxin *p*-azidobenzoic acid.

**Synthesis of VI:** [Brevetoxin PbTx-3-*p*-azidobenzoic acid]. Either labeled or unlabeled *p*-azidobenzoic acid may be used for the synthesis, and either tritiated or unlabeled brevetoxin may be used. The reaction is carried out under red light to avoid photoactivation of the probe during synthesis. The reaction sequence is initiated by mixing equimolar carbonyldiimidazole and *p*-azidobenzoic acid in minimal volume of benzene. PbTx-3 was coupled to the photoprobe by mixing 0.1 mole equivalent of toxin and heating in a sealed glass tube for 24 hours at 70°C. Following reaction, the mixture was separated on preparative silica gel tlc plates using acetone:petroleum ether (30:70) as mobile phase. The complete brevetoxin photoaffinity probe (VI) migrated with an  $R_f$  of 0.40 and was eluted from the plate with acetone. Alternatively, complete probe can be separated from side products using reverse phase high pressure liquid chromatography (C-18, 85% isocratic methanol, detection at 215 nm.).

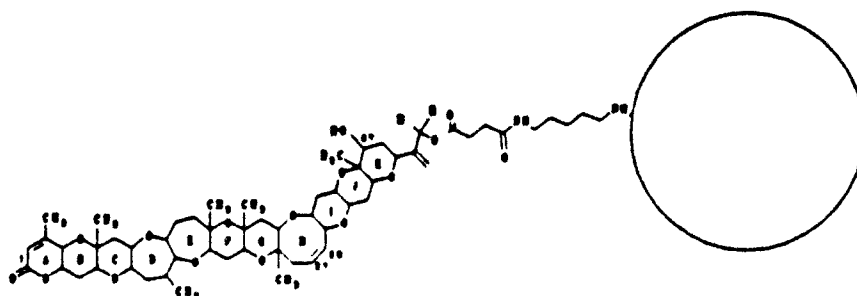


Figure 11. Brevetoxin aminobexyl Sepharose.

**Brevetoxin Affinity Columns.** For construction of affinity columns, aminobexyl Sepharose was used as solid support matrix. Purified PbTx-3 was dissolved in minimal redistilled pyridine and was succinylated with 10-fold molar excess of succinic anhydride at 80°C for 2 hours. Following separation of unreacted PbTx-3 and succinate reagent from toxin-succinate by tlc (silica gel, 70/30 ethyl acetate/petroleum ether), the free carboxyl function was covalently coupled to the free amino functions on the AH Sepharose using standard carbodiimide coupling procedures [13]. Following coupling, the solid support matrix was placed in a small column, and was sequentially washed with 50% aqueous pyridine, ethanol, methanol, and water. Based on the stoichiometry of the AH Sepharose, and the amount of brevetoxin succinate recovered, approximately 3-4 amoles were bound per mL of gel---as compared to a theoretical maximum of 4-6 amoles per mL available coupling sites.

**Tetrodotoxin Modifications.** The structure for tetrodotoxin is shown below in figure 12. As illustrated, the C-6 and C-11 functionalities are the focus of our derivatization attempts. In order to produce the desired derivatives, our strategy is to employ a number of protection steps, followed by selective de-protection and derivatization, followed by total deprotection to yield the appropriate derivatives. Our progress on tetrodotoxin is summarized below.

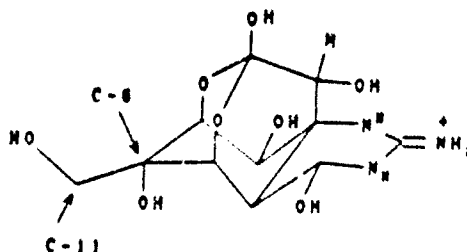


Figure 12. Tetrodotoxin, illustrating the C-11 and C-6 functionalities to be exploited in Derivatives.

Our initial task was to protect the C-11 primary hydroxyl function with a labile protecting group. We investigated the use of four different primary protecting groups, each with a different ease of removal following synthesis. These four protecting groups include triphenylmethyl chloride (trityl chloride), di-*p*-methoxy-trityl chloride, trimethoxytrityl chloride, and *t*-butyldimethylsilyl chloride.

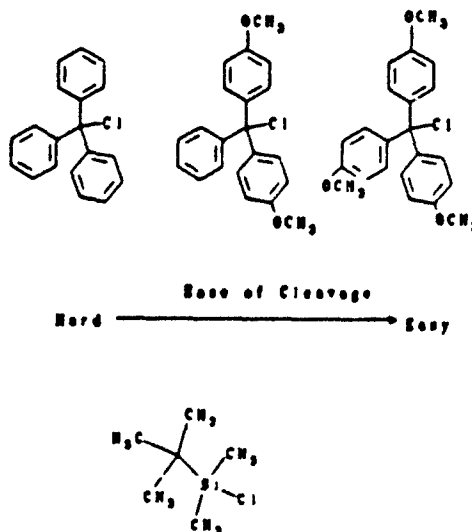


Figure 13. Protecting groups for primary alcohol on tetrodotoxin. From left to right: trityl chloride, dimethoxy trityl chloride, trimethoxy trityl chloride. The ease of cleavage increases from left to right. *t*-butyldimethylsilyl chloride is indicated below the arrow, and is intermediate in ease of cleavage as indicated by its position on the cleavage arrow.

Trityl (or dimethoxy- or trimethoxy-) chloride was reacted with tetrodotoxin in stoichiometric amounts or 5% excess trityl derivative in dry pyridine. Reactions were carried out at room temperature for 48 hours, at 70° C for 2 hours, at 100° C for 2 hours, at 108° C for 2.5 hours, or 85° C overnight. A variation of the procedure involved using 0.4 mole equivalents of dimethylaminopyridine as catalyst and 1.1 mole equivalents of triethylamine as an acid scavenger, with either dichloromethane, dimethylformamide, or dimethylsulfoxide as solvents. These were poured onto ice water and extracted with dichloromethane, and the organic layer washed with saturated ammonium chloride and water.

Tertiary butyl silyl derivatization was attempted using 5% molar excess reagent, and reacting with tetrodotoxin using dimethylaminopyridine and triethylamine in dichloromethane; in some cases, a small addition of hexamethylphosphoramide was added to increase solubility of tetrodotoxin in solvent. Reactions were run for similar time frames and temperatures as listed above for trityl derivatives. Derivatization at this point occurs solely at the primary hydroxyl, as illustrated with the dimethoxytrityl derivative in figure 14 below.

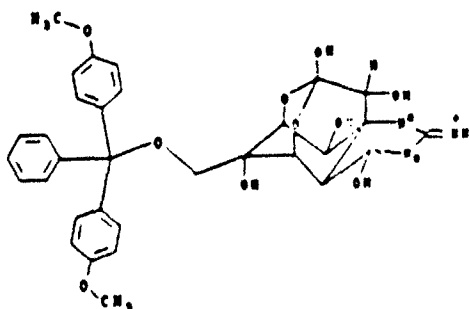


Figure 14. Dimethoxytrityl tetrodotoxin.



Once the primary hydroxyl function was protected, we benzylated the remaining unprotected secondary hydroxyls, to produce *t*-butyl dimethylsilyl (used for this step thus far) -benzyl tetradotoxin (tBDMS-TTX) (illustrated as the dimethoxybenzyl derivative in figure 15a). The tBDMS-TTX was treated with excess benzyl bromide and silver oxide (used as catalyst) in dimethylformamide, and incubated at room temperature with shaking for four days. The reaction mixture was streaked on a 250  $\mu$ m silica gel plate and chromatographed with 50:50 ether: hexane as mobile phase. The derivatized fraction ( $R_f$  0.95) was eluted and flash evaporated. The resultant crystals were pressed into KBr for infrared analysis. Following analysis, the tBDMS group was removed by hydrolysis for 72 hours in 0.1M acetic acid:water:tetrahydrofuran (3:1:1) (figure 15b). This material was sent off for elemental analysis.

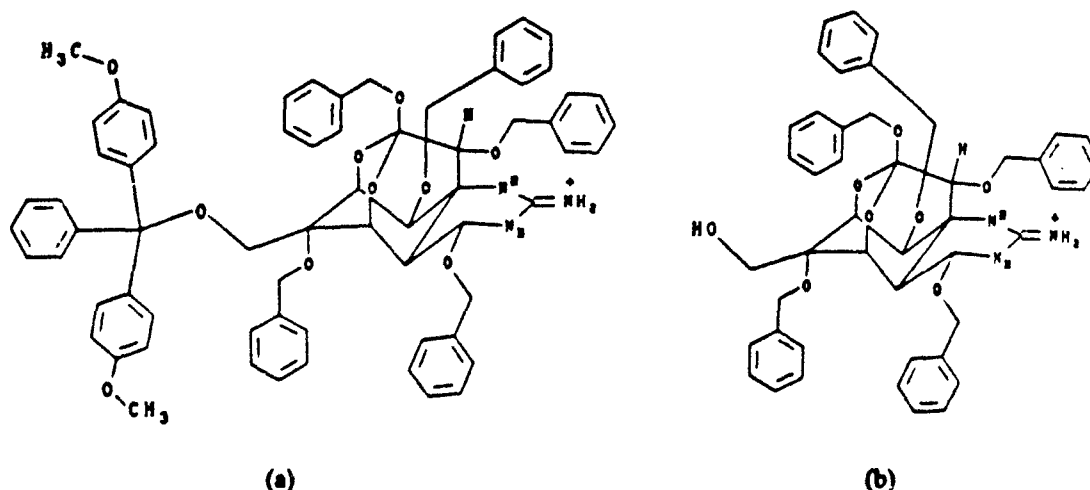


Figure 15. Dimethoxytrityl-benzylated tetradotoxin (a), and deprotected benzyl tetradotoxin (b).

Oxidation of the primary hydroxyl functionality in tetradotoxin to the aldehyde, in preparation for re-reduction to tritiated tetradotoxin (figure 16) using sodium borotritide, was accomplished by reacting with dicyclohexylcarbodiimide and orthophosphoric acid in anhydrous dimethylsulfoxide. Prior to its addition, the TTX was dissolved in 0.5% trifluoroacetic acid to increase its solubility during reaction. The mixture was heated for 4 hours at 40°C in a sealed vessel, converting the alcohol to the aldehyde. The mixture was filtered and the filtrate retained. The filtrate was washed with diethyl ether and centrifuged. The precipitate was redissolved in solvent and spotted on a filter pad. Upon reaction with dinitrophenylhydrazine, a characteristic aldehyde-positive color reaction was visible.

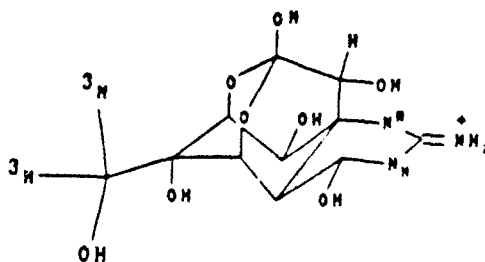


Figure 16. Tritiated tetradotoxin arising from re-reduction of aldehydetetradotoxin.

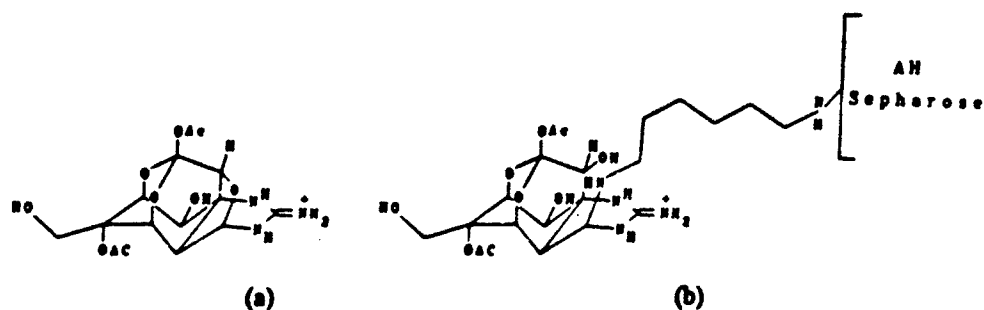


Figure 17. Anhydroepitetrodotoxin and aminohexyl tetrodotoxin amide.

Tetrodotoxin was reacted with *p*-toluene sulfonic acid and acetic anhydride, producing tetraacetylanhydroepitetrodotoxin (figure 17 a). Aminohexyl Sepharose was swelled in deionized water, washed with 10% NaOH followed by distilled water, and was then added to the tetra-acetylanhydroepitetrodotoxin and incubated at room temperature for 7 days. The resulting derivative (figure 17 b) Sepharose was poured into a small glass column, and exhaustively washed with distilled water, followed by 1 M sulfuric acid and finally water. Each fraction was tested for the presence of TTX by the nitroferrocyanide-peroxide color reaction. Columns were stored in pH 7.4 PBS containing 0.01% sodium azide.

**Saxitoxin Derivatives.** Saxitoxin for our derivatization effort is supplied by the U.S. Army Medical Research and Development Command in Fort Detrick, and is used without further purification (figure 18).

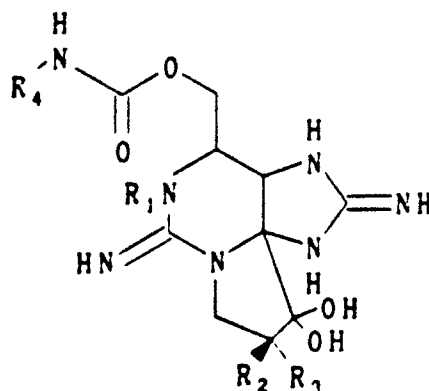


Figure 18. Saxitoxin

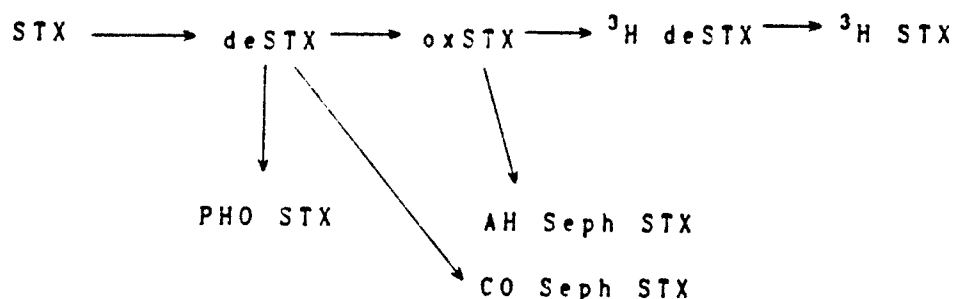


Figure 19. Progression for STX organic manipulations.

As with the brevetoxins and with tetrodotoxin, our principal efforts are aimed at developing toxin affinity columns, non-exchangeable tritiated toxins, and photoaffinity probes of saxitoxin. In terms of saxitoxin, one area of the molecule which appears quite attractive for derivatization without decreasing potency, is the  $R_4$  region of STX. Each of the derivatives we are pursuing manipulates the carbamoyl portion of STX as the initial step. This is indicated above in figure 19. A second effort is the total synthesis of saxitoxin following the method of Kishi *et al.* [19].

Saxitoxin (1 mg) was dissolved in 0.25 mL 7.5 M HCl, sealed in a thick-walled glass tube, and heated at 110°C for three hours to produce decarbamoyl saxitoxin (figure 20) [20]. A brown residue resulted, and was reduced to dryness using a stream of nitrogen. The residue was re-dissolved in alcohol and applied to an alumina column prepared in a Pasteur pipet, and eluted with ethanol. The resulting decarbamoyl saxitoxin was chromatographed on small fluorescent tlc (5 x 10 cm) silica gel plates using pyridine/ethyl acetate/water/acetic acid (15/5/4/3) as mobile phase against authentic saxitoxin. The plate was sprayed with 1% hydrogen peroxide and was heated at 105°C for 30 minutes. Fluorescent patterns and migrations were compared using a 366 nm uv light.

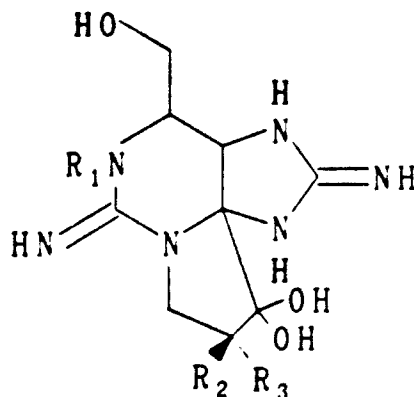


Figure 20. Decarbamoyl saxitoxin.

We have also begun the total synthesis of saxitoxin and the first few steps are illustrated in figure 21 below. Beginning with the Bunte salt, step one proceeds by mixing 125 g sodium thiosulfate pentahydrate with 259 mL water, 0.2 moles (40g) 1,3 dibromopropane and 250 mL 95% ethanol. These reagents were reacted under refluxing conditions until the solution was homogeneous. Following cooling, the solvent was flash-evaporated and dried over KOH. The crystals which resulted were dissolved in ethanol and were heated to boiling and then filtered. This was repeated twice more, the soluble derivative in ethanol being combined. The filtrates were flash-evaporated and dried over KOH.

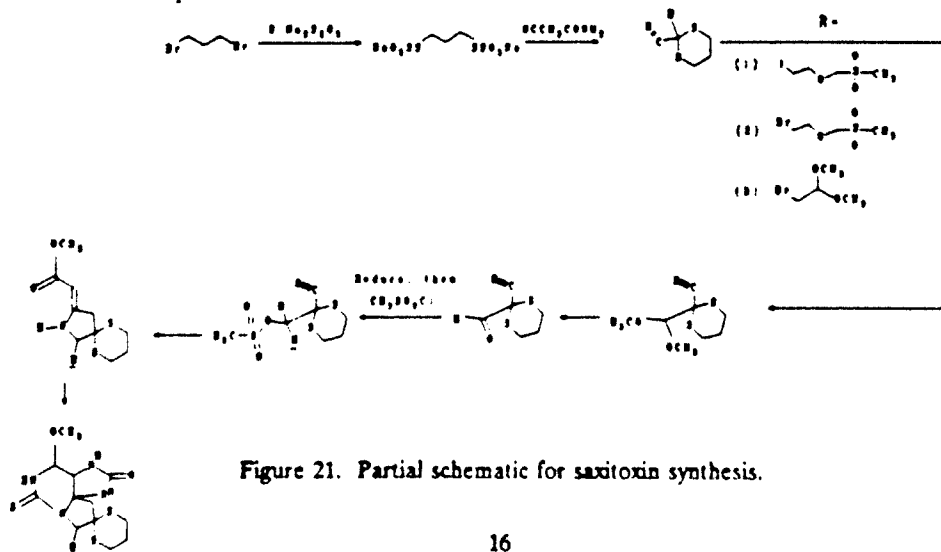


Figure 21. Partial schematic for saxitoxin synthesis.

The dried Bunte salt from step 1 was dissolved in DMF, and to this solution was added 2.11 g cyanoacetamide. The mixture was stirred and 1.8g sodium hydride was added under nitrogen atmosphere in a glove bag. The complete reaction mix was stirred for 13 hours and was then poured into 500 mL distilled water under stirring conditions. The aqueous solution was extracted twice with diethyl ether, and the ether layer was flash evaporated. The residue was recrystallized from 50% ethanol, yielding white needles (mp 89°C). Crystalline material was dried over phosphorus pentoxide.

The preparation of the cyanomesylate (steps 3,4, and 5) has been approached using three different protocols. These three were attempted, due to the difficulty in repeating the yields obtained by Kishi using compound (1). The method used for the protocols (substituting (1) for (2) for (3) as applicable) is as follows: 1 g of 2-cyano-1,3-dithiocyclohexane was dissolved in 40 mL dry THF at -25°C under nitrogen. Four mL of 2 M LDA was slowly added and allowed to react for 2 hr at temperature. Ethylene oxide (0.4 mL) was added and allowed to react one hr and then overnight at -20°C. The solution was streaked on a preparative thin-layer silica gel plate and was chromatographed using hexane/ether (40/60). A band with  $R_f$  0.1-0.25 was scraped and eluted with ether. The product was dried and redissolved in 100 mL dichloromethane at -25°C under a nitrogen atmosphere. To this was added 24 mL triethylamine and 12 mL mesyl chloride ( $\text{CH}_3\text{SO}_2\text{Cl}$ ) slowly. A dark oil separates and is removed in a separatory funnel, plated in the same solvent system as above, and a band with an  $R_f$  of 0.1-0.2 is isolated.

**Brevetoxin Binding Site.** Investigation employed synaptosome preparation, Rosenthal analysis of photoprobe, sodium dodecyl sulfate polyacrylamide gel electrophoresis, binding site solubilization and gel filtration, chemical and proteolytic cleavage of photoprobe-bound synaptosomes, Bio-Bead SM2 purification, Bligh and Dyer [21] extraction, ion exchange and wheat germ agglutinin-sepharose chromatography, immunoprecipitation of bound material, phosphorylation studies with  $\text{Na}^+$  channels, and  $^{32}\text{P}$  radioimmunoassay.

(1) Preparation of synaptosomes. Frozen rat brains are purchased from Harlan-Sprague Dawley Co and are homogenized and prepared according to Dodd *et al.* [22], and are used at a concentration of 0.1 mg/mL for binding experiments. Reactivity is retained at -80°C for 6 months.

(2) Binding experiments (Rosenthal analysis). Binding of tritiated PbTx-3-azido probe was determined using a rapid centrifugation technique [14]. Synaptosomes are added to reaction vials containing tritiated PbTx-3-photoprobe. Nonspecific binding is determined in the presence of 10  $\mu\text{M}$  unlabeled toxin-photoprobe. After mixing and incubating for 1 hr at 4°C in the dark, samples are centrifuged for 2.5 min at 15,000  $\times$  g. Supernatant solutions are sampled for free [ $^3\text{H}$ ] PbTx-3-Pho and pellets are washed with three drops of ice cold wash medium containing 5 mM HEPES (pH 7.4), 163 mM choline chloride and 1 mg/mL BSA. Pellets are transferred to counting vials and bound radioactivity determined by scintillation spectrometry. All phases of Photoaffinity Rosenthal experiments are carried out under red light or in the dark.

(3) SDS-PAGE. Sodium dodecyl sulfate polyacrylamide gel electrophoresis is carried out following the photoaffinity protocol. A one hour incubation of the reaction mixtures at 4°C is followed by transfer to a petri dish and irradiation at a distance of 1 cm for 10 minutes (254 nm). Samples are centrifuged at 4°C in a microfuge, supernatant samples are taken, and the pellets are washed with three drops of ice-cold wash medium [14]. Pellets are prepared for SDS-PAGE by resuspension in sodium dodecyl sulfate sample buffer [22], and incubation at 100°C for 2 min. Samples are loaded on 1.5 mm thick SDS acrylamide gels prepared by the method of Blatter *et al.* [23]. Solubilized photoaffinity-toxin-sodium channel (NaTPHO) are run through the stacking gel at 75 mV and at 200 mV through the resolving gel. Gels of 5%, 10%, and 15%, and gradient gels of 5-15% were run. After electrophoresis, gels were stained with 2% Coomassie brilliant blue for one hr, then destained to locate protein bands [24]. Gels were sliced into 1 mm thick pieces with a razor blade, and molecular weights checked against marker standards. Slices were dissolved in Soluene (Packard Instruments) and 0.1 mL water at 60°C for 3 hr. Glacial acetic acid was added to neutrality. Six mL scintillant was added to each vial, and radioactivity was assessed.

(4) Synaptosome solubilization and gel filtration. Following irradiation with uv light as described above, NaTPHO was solubilized according to ref [24]. Over a period of 30 min at 4°C, aliquots of 4% triton X-100 were added until a 2% solution was obtained. Unsolubilized material was sedimented by centrifugation at 110,000  $\times$  g, and the supernatant solution was carefully decanted. One mL aliquots were loaded on a calibrated Sephacryl S-300 column (Pharmacia). Modified mobile phase [24] containing 25 mM  $\text{CaCl}_2$  and 0.2 M NaCl was used to size fractionate the photoaffinity bound material. One half mL fractions were collected and assayed for tritium counts and protein.

(5) 2-mercaptoethanol treatment. This method was run according to the method of Sharkey *et al.* [6]. One mL of the fraction from procedure (4) (est MW 316,000) above is recovered from the Sephacryl column and was incubated for 4 min at 100°C with 15 mM 2-mercaptoethanol. Forty five mM iodoacetamide in 0.1 M

## Results

**Brevetoxin binding site characterization.** The p-azidobenzoyl photoaffinity probe has been determined by C-18 reverse phase HPLC analysis to be stable for at least 6 months when stored in 100% ethanol at 0°C. A Rosenthal analysis of photoaffinity probe binding to nerve membrane resulted in a non-linear plot, suggesting the presence of two binding sites for the brevetoxin molecule on the Na<sup>+</sup> channel (Fig. 22). Binding of the photoaffinity label to the high affinity site resulted in a  $K_d$  of 0.64 nM and  $B_{max}$  of 3.74 pmole/mg. The low affinity site binding characteristics ( $K_d$  = 2.65 nM,  $B_{max}$  = 6.8 pmole/mg) are similar to those derived by Poli *et al.* (1986) for native PbTx-3. Evidence supporting two site binding of brevetoxin to nerve membranes has become apparent in Rosenthal analyses of native [<sup>3</sup>H]PbTx-3 binding to rat brain synaptosomes.

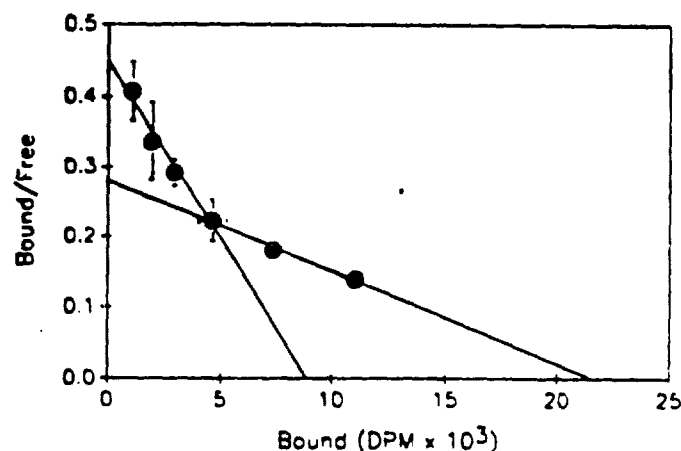


Figure 22. Rosenthal analysis of tritiated PbTx-3-photoaffinity probe to rat brain synaptosomes. Concentrations ranged from 0.78 to 25 nM tritiated toxin probe. Unlabeled photoaffinity probe concentration was 10  $\mu$ M. High affinity site:  $K_d$  = 0.64 nM,  $B_{max}$  = 3.74 pmol/mg protein. Low affinity site:  $K_d$  = 2.65 nM,  $B_{max}$  = 6.8 pmol/mg protein.

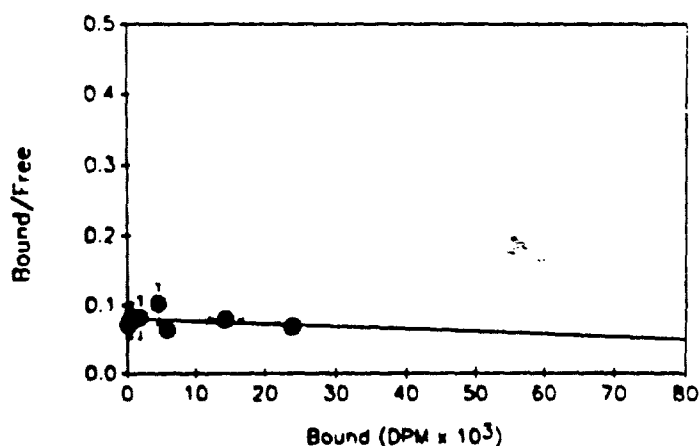


Figure 23. Rosenthal analysis of tritiated PbTx-3-photoaffinity probe to rat brain synaptosomes pre-incubated with 5 nM unlabeled toxin-photoaffinity probe.

To characterize brevetoxin binding at the low affinity site alone, synaptosomes were incubated first with 5 nM cold PbTx-3-photoprobe to saturate binding at the high affinity site. A Rosenthal analysis was carried out (Fig. 23). The pre-treated synaptosomes displayed only low affinity binding.

*Optimizing brevetoxin photoaffinity probe covalent modification of sodium channels.* Characterization of photoaffinity probe binding to synaptosomes was carried out to determine the optimal UV irradiation time which resulted in maximal total binding. An increase in total binding with irradiation times up to 10 min. was observed. A increase in nonspecific binding from the zero time (no irradiation) value is attributable to the hydrophobic nature and highly active nitrene group of the photoaffinity probe. This elevated nonspecific binding is a common problem encountered when working with photoaffinity labels which can be minimized by using one or more scavengers (see below).

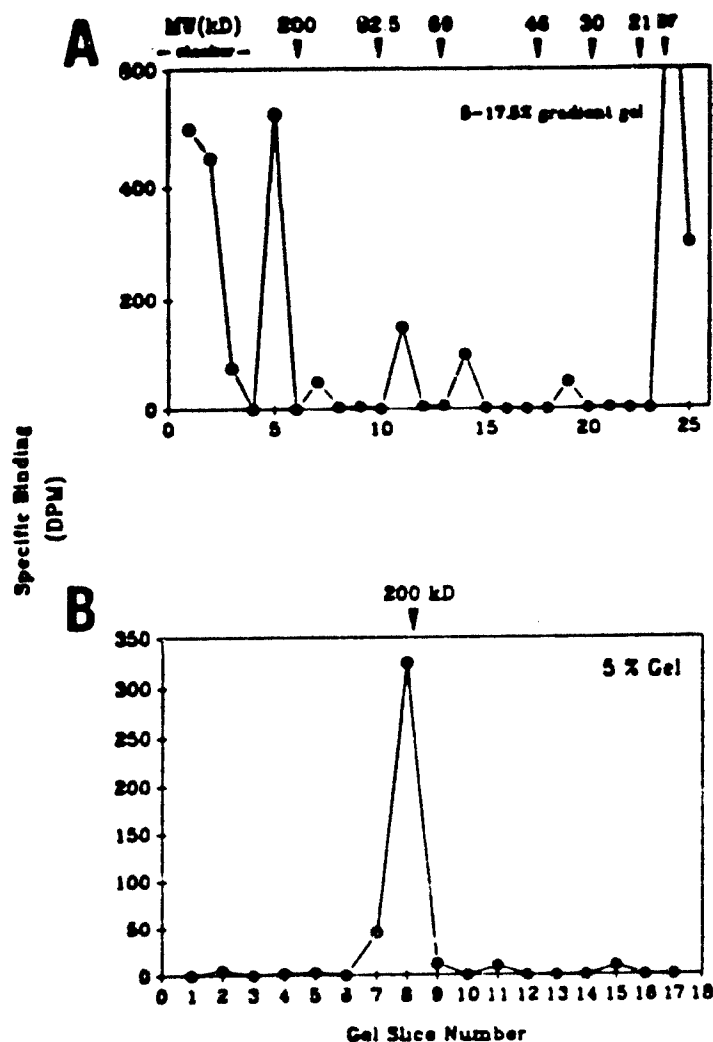


Figure 24. SDS-PAGE analysis of synaptosomes binding to [ $^3\text{H}$ ] PbTx-3-photoprobe on a 5-17.5% gradient gels (panel a), or 5% gels (panel b). Non-specific binding (in parallel lanes with 10  $\mu\text{M}$  cold toxin-photoprobe) was subtracted from total binding to yield specific binding. MW standards were run in gels and are indicated on the top of panel a and the 200 kD marker in panel b.

SDS-PAGE of [ $^3\text{H}$ ]PbTx-3-photoprobe covalently bound to synaptosomes was performed using both a 5-17.5% gradient gel and a 5% acrylamide gel. The gradient gel was used to resolve binding of the photoaffinity probe to both the  $\alpha$ - $\beta$  2 subunit complex (about 300 kD) and the  $\beta$  1 subunit (39 kD) on the same gel. A protein band with a molecular weight slightly greater than 200 kD was determined to contain the most specifically bound radioactivity (Fig.24a). Since this band was located in such close proximity to the stacking gel which also contained radiolabelled proteins, a 5% gel was used to separate these two components and to provide further evidence that the  $\alpha$ - $\beta$  2 complex binds the radiolabelled photoaffinity probe (Fig.24b).

The high degree of nonspecific binding which was observed in studies using the photoaffinity probe made it necessary to use a protein scavenger. This molecule is used to provide multiple reaction sites for nonspecifically reacting photoproducts. Binding medium containing 1% BSA as a scavenger protein was used to successfully decrease nonspecific binding by 22%. Three washes by centrifugation prior to photolysis resulted in a increase in specific binding to 86%. All binding experiments utilizing the photoaffinity label take advantage of three pre-UV washes with BSA and a 5-10 minute irradiation time.

SDS-PAGE analysis of [ $^3\text{H}$ ]PbTx3-Pho binding to synaptosomes was not easily analyzed due to high chemifluorescence (contributing to high background) caused by acrylamide during scintillation spectroscopy. It was also difficult to precisely match Coomassie-stained lanes of total and nonspecific binding and to cut equally-sized pieces of gel. To support gel electrophoresis results, similar experiments were performed and analyzed by gel filtration.

Gel filtration studies supported findings obtained by SDS-PAGE. Under non-reducing conditions, a single protein peak of specifically bound radioactivity (Fig.25) was eluted from the Sephacryl column at a Mr of about 316 kD (Fig. 26).

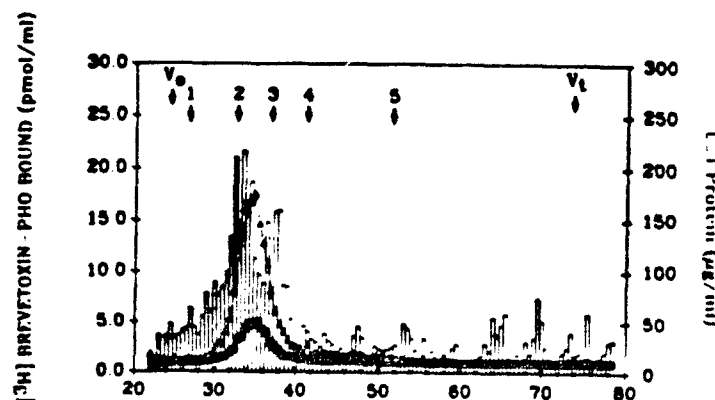


Figure 25. Sephacryl S-300 gel filtration of brevetoxin receptor under non-reducing conditions. Void volume = 24 mL, Total volume = 74 mL. MW standards are: (1) thyroglobulin (669 kD), (2) ferritin (440 kD), (3) catalase (232 kD), (4) aldolase (158 kD), (5) ovalbumin (43 kD). DPM migration does not change under  $\beta$ -mercaptoethanol treatment.

This brevetoxin-binding protein has a calculated Stokes radius of approximately 50 Å (Fig.27). These results strongly suggest that [ $^3\text{H}$ ]PbTx3-Pho binds to a portion of the  $\alpha$ - $\beta$  2 Na<sup>+</sup> channel subunit complex. Two-mercaptoethanol cleavage of the  $\alpha$  subunit from the disulfide-linked  $\beta$  2 resulted in retention of binding at the high molecular weight protein band. Although specific binding appears to have been retained at the  $\alpha$  subunit, a peak of "nonspecific" binding became evident. The elution volume (V<sub>e</sub>) of this peak corresponds to the approximate Mr expected for the dissociated  $\beta$  2 subunit. It is possible that the high concentration of unlabelled PbTx3-Pho resulted in a conformational change of the receptor, thereby displacing [ $^3\text{H}$ ]PbTx3-Pho from its high affinity binding site (probably located on the  $\alpha$  subunit) to a low affinity site located on the  $\beta$  2 subunit. This result correlates with Rosenthal analyses which revealed a two-site binding characteristic of brevetoxin with its Na<sup>+</sup> channel receptor.

Further treatment of column fractions showed that glycoproteins are not involved in the interaction of brevetoxin photoaffinity probe with the Na<sup>+</sup> channel. Neither cleavage of terminal sialic acids using

neuraminidase (Fig. 28) nor removal of high mannose and complex glycans with endoglycosidase F (endo F; Fig. 29) resulted in a change in elution characteristics of the brevetoxin-binding protein. The higher  $M_r$  of the protein treated with endo F is probably an artifact caused by the high SDS content of the buffer. This hypothesis will be tested by SDS-PAGE analysis of all proteins subjected to chemical and proteolytic cleavage and direct comparison with standards of known molecular weights.

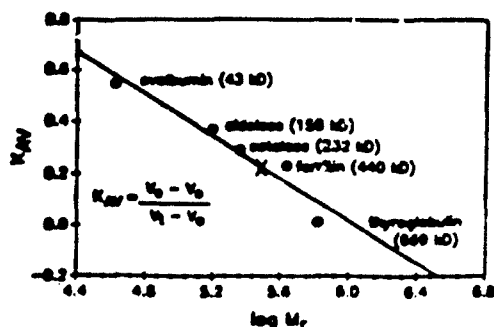


Figure 26. Molecular radius determination of brevetoxin receptor. Sephacryl S-300 elution as indicated in figure 25.

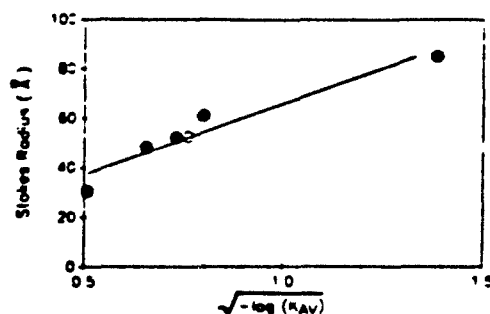


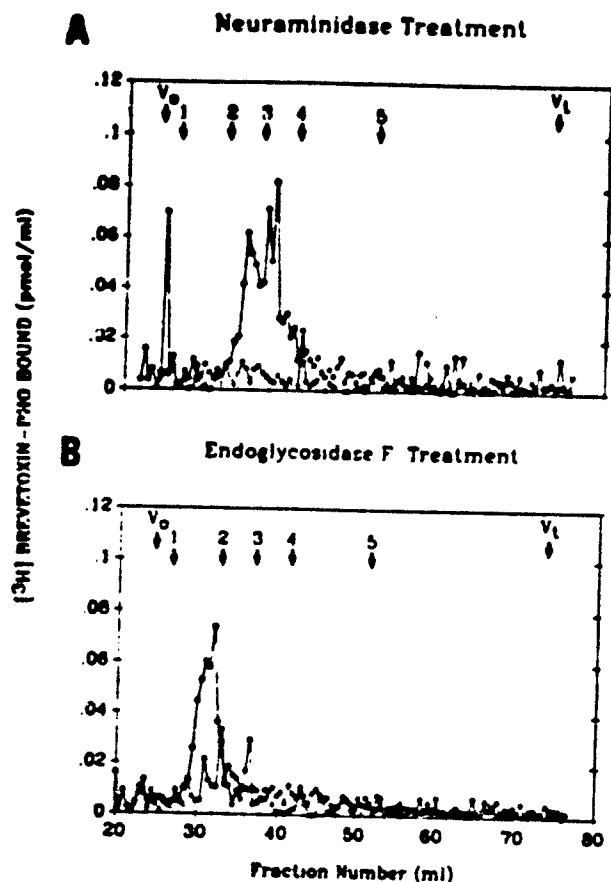
Figure 27. Stokes radius calculation.

**Optimizing brevetoxin photoaffinity probe binding.** The UV activation reaction of the p-azido benzoate brevetoxin derivative resulting in its covalent linkage to synaptosomal nerve membranes was further optimized. Through spectral analysis of UV irradiated p-azido benzoic acid, it was determined that 30 sec exposure to 254 nm light was effective in completely activating the compound. The 366 nm light required more time to activate the photoaffinity probe. Gel electrophoretic analysis of synaptosomes exposed to 0.5 to 20 min of UV light showed that up to 10 min irradiation of this protein was possible without visible crosslinking problems (determined by visual inspection of Coomassie-stained gels). Five min was chosen to maximize irradiation time for activation of the photoaffinity probe without excessive protein cross-linking.

In an attempt to further purify the NaTPHO, the eluent from the gel filtration column was prepared for application to WGA-Sepharose by removal of Triton X-100. Several methods of detergent removal were tested. Polystyrene beads (Bio-Beads SM-2; Bio-Rad), which had been shown to bind hydrophobic detergent molecules, also bound the sodium channel-toxin complex since the conjugate had taken on the lipophilic characteristic of the covalently-bound brevetoxin. A Bligh and Dyer [26] separation gave similar results, i.e., all [ $^3H$ ] conjugate activity was found in the hydrophobic chloroform fraction.

Sucrose gradient centrifugation resulted in a coincidental peak of protein and [ $^3H$ ] brevetoxin radioactivity, but the NaTPHO appeared to be much less dense than underivatized sodium channel (fig 30). Due to the tedious, time-consuming nature of this assay, it was not used as a method of purification prior to the WGA-Sepharose step.





Figures 28 and 29. Gel filtration of the modified brevetoxin receptor. Sephacryl S-300 size chromatography after biochemical modification of tritiated photoaffinity probe-brevetoxin sodium channel  $\alpha$ -subunit. Panel A = post-neuraminidase treatment as described in text; Panel B, post-endoglycosidase F treatment as described in text. Closed circles are total binding, open circles non-specific binding. Molecular weight standards are marked 1-5, as described in figure 25.

The most viable method of Triton X-100 removal was ion exchange chromatography. Due to the nonionic nature of this detergent, it did not bind to the DEAE Sephadex A-25 column, whereas the charged sodium channel molecules remained tightly bound until displaced by a cationic buffer. Previously published work had shown that 0.25 M KCl was sufficient to displace sodium channel protein from this column. The photoaffinity-labeled sodium channel bound more tightly, however, and 1 M KCl was required for its complete dissociation from the ion exchange column. The elution profile of NaTPHO from a DEAE Sephadex A-25 column is shown in Fig. 4. The eluent from this column was directly adsorbed to a WGA-Sepharose column and eluted using 0.3 M NAG (Figs. 31 and 32).

The tritiated brevetoxin receptor was purified almost 7-fold through the lectin-affinity column step (Table 2). Previously published purification of the sodium channel has been shown to be much greater when taken through the same steps [24]. In this study, however, the toxin is bound to its sodium channel receptor prior to purification. The apparent lower purification was probably due to the dissociation of non-covalently bound brevetoxin during the extensive wash steps.

In preparation for immunoprecipitation studies, the PbTx-Pho NaCh was treated with varying concentrations of TPCK-trypsin and filtered through polysulfone centrifugation filters (Millipore) to determine the size of peptide fragments. Apparently, 1 mg/ml trypsin was needed to give a range of peptides useful for

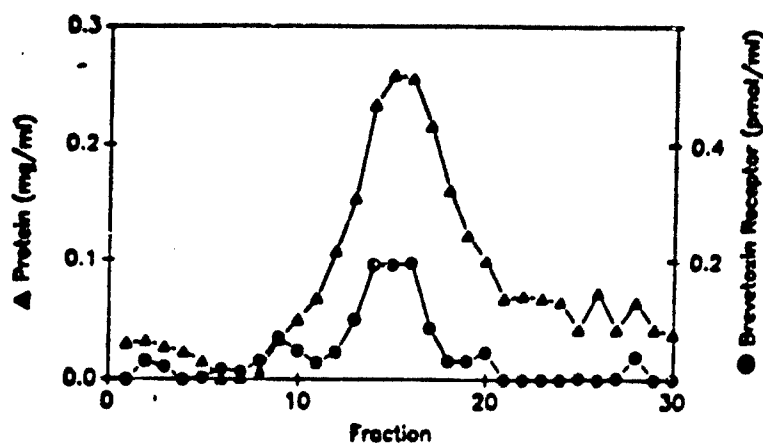


Figure 30. DEAE-Sephadex A-25 chromatography. Profile of half ml fractions of NaTPHO eluted with 1 M KCl from a DEAE Sephadex A-25 column. Protein was measured by the method of Bradford using BSA as a standard. Brevetoxin receptor activity was measured as the difference in radioactivity between columns adsorbed with NaTPHO alone and with the addition of a 1000-fold excess of unlabeled PbTx-3.

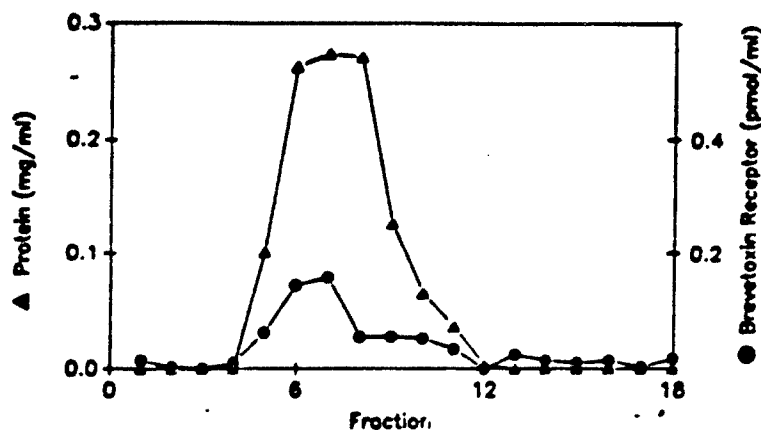


Figure 31. Wheat germ agglutinin chromatography. Profile of 1 ml fractions of PbTx-Pho NaCh eluted with 0.3 M NAG from a WGA-Sepharose column. Protein and brevetoxin receptor activity were analyzed as in Fig. 30.

immunoprecipitation studies (figure 32). This enzyme concentration was 10-100 fold higher than that shown by other investigators to give similar cleavage patterns. The Triton X-100 remaining in the purified samples was bound to the tryptic fragments, resulting in falsely high estimates of their molecular size.

Gel slices of trypsinized NaTPHO subjected to SDS-PAGE were used as an alternative to the filtration assays. These experiments showed that a 1 min incubation with 10  $\mu$ g/ml TPCK-trypsin resulted in a complete range of peptides useful for immunoprecipitation studies (Fig. 33). Treatment with 100  $\mu$ g/ml TPCK-trypsin resulted in a majority of peptides smaller than 46 kD after only 1 min digestion (Fig. 34).

Prior to the initial immunoprecipitation experiments, the NaTPHO preparation was compared to  $^{32}$ P sodium channel synthesized in Catterall's laboratory. It was apparent that the peak of [ $^3$ H] brevetoxin binding (determined by gel slicing) coincided with the major band corresponding to phosphorylated  $\alpha$  subunit of the sodium channel (determined by autoradiography; Fig. 35). These results further supported evidence that brevetoxin specifically binds to the sodium channel  $\alpha$  subunit.

Rabbit antibodies against conserved peptide sequences from the four separate sodium channel domains were assayed for activity by RIA. Anti-SP1,  $\alpha$ -SP14,  $\alpha$ -SP29 all showed high affinity for their sodium channel

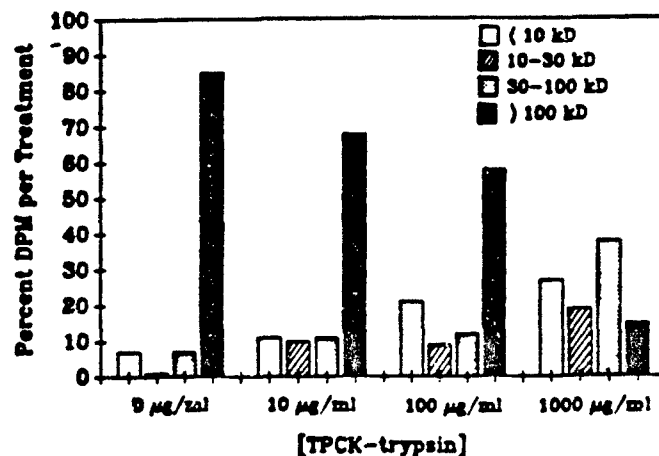


Figure 32. Brevetoxin receptor trypsinization. Analysis of NaTPHO digested by incubation with TPCK-trypsin at the designated concentrations. Size of fragments was analyzed by centrifugation through Millipore filters with 10 kD, 30 kD, 100 kD nominal molecular weight cutoffs. Samples were centrifuged at less than 5000 RPM in a microfuge until the filter was almost dry. The filter was rinsed once with a small amount of Buffer S, then centrifuged to dryness. Filters were assayed for radioactivity.

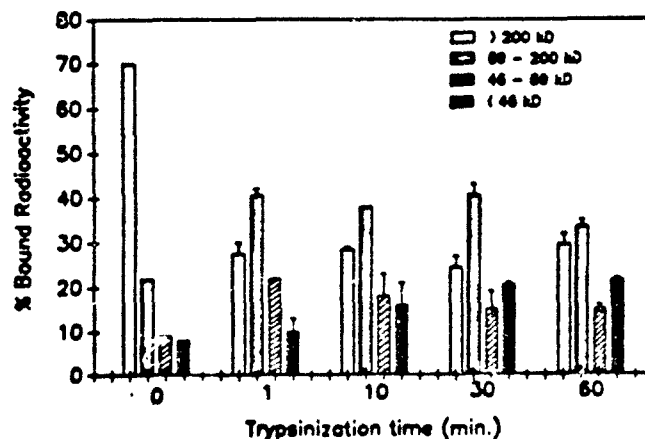


Figure 33. SDS-PAGE analysis of NaTPHO treated with 10 µg/ml TPCK-trypsin. Gel lanes were sliced into approximately 4 mm pieces, compared to molecular weight standards and assayed for radioactivity.

receptors, whereas  $\alpha$ -SP35 was shown to be an antibody with weak affinity for its receptor. Results obtained using the latter antibody were not documented due to low sample radioactivity.

The first immunoprecipitation experiment utilized  $\alpha$ -SP1 and intact (non-digested) PbTx-Pho NaCh. Two different concentrations of  $\alpha$ -SP1 showed significant recognition of the brevetoxin-linked sodium channel protein over the preimmune serum control. Tryptic digestion of the tritiated sodium channel conjugate for 1, 10 or 60 min showed that only the domain IV antibody ( $\alpha$ -SP29) retained greater than 60% of its control binding activity at the final time point (Fig. 36). When this experiment was repeated using an additional domain IV antibody, ( $\alpha$ -SP13), the results were similar (Fig. 37), showing that both of the domain IV antibodies recognized the tryptic peptide containing the brevetoxin receptor.

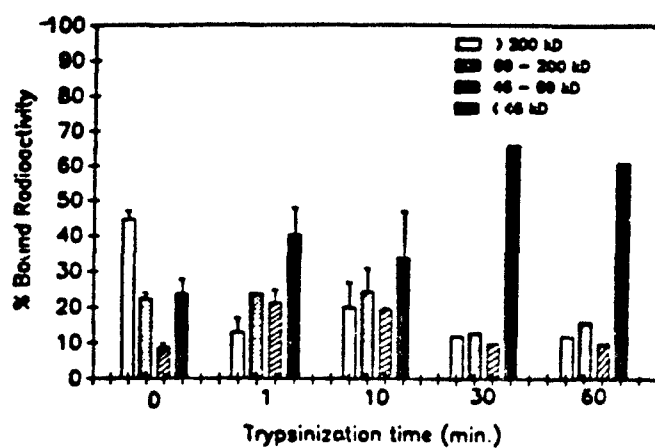


Figure 34. SDS-PAGE analysis of NaTPHO treated with 100 µg/ml TPCK-trypsin. Treatment identical to figure 33.

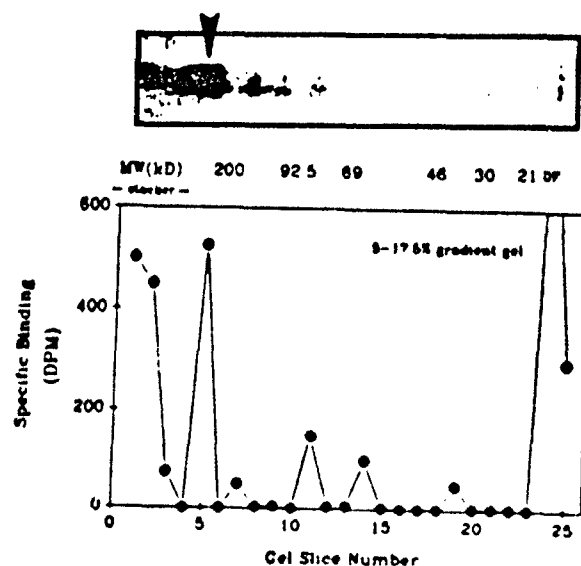


Figure 35. SDS-PAGE comparison of  $^{32}\text{P}$ -labeled and brevetoxin photoaffinity labeled  $\alpha$ -subunit of sodium channel. The  $\alpha$ -subunit is indicated in the gel by an arrow.

Further work, using photoaffinity probe which is synthesized using the tritiated aromatic ring of the benzoate function, should yield probes with higher specific activities and hence more counts in each lane of gels treated with enzymes. We expect this work to succeed by late Fall of 1990.

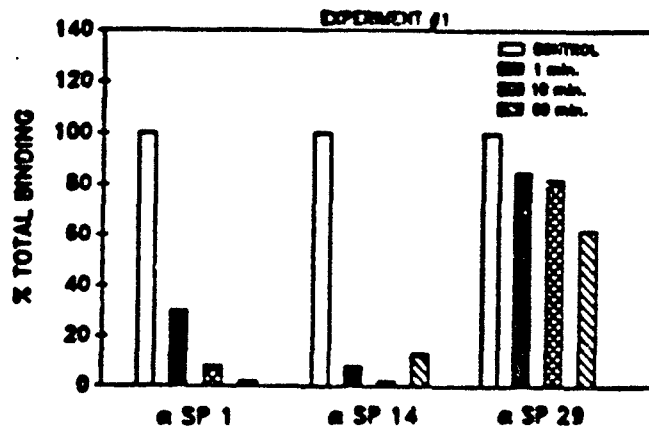


Figure 36. Trypsinization time course and immunoprecipitation using antibodies directed against peptides of the four sodium channel domains. Each point is a single determination.

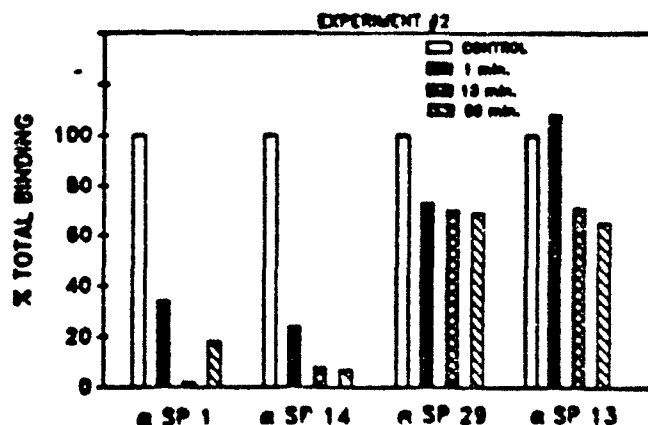


Figure 37. Confirmation of Domain 4 using anti-SP13 antibodies. Same protocol as figure 36.

Specific domains of each of the antisodium channel antibodies elucidated by Catterall's group have aided in determining that the brevetoxin photoaffinity probe binds with a 1:1 stoichiometry with the  $\alpha$ -subunit of the VSSC. The specific domain for brevetoxin binding is domain IV. Both  $\alpha$ -SP29 and  $\alpha$ -SP13 specifically immunoprecipitate tritiated counts in NaTPHO trypsin digests. These two antibodies specifically recognize the extracellular hydrophobic loop between membrane peptide units S5 and S6 of domain IV. Other antisodium channel antibodies which failed to bring down tritiated brevetoxin photoprobe counts were  $\alpha$ -SP1 (specific for intracellular loop between S4 and S5 of Domain I) and  $\alpha$ -SP 14 (specific for extracellular loop between S5 and S6 of Domain III). Further work, isolating the specific peptides, and sequencing to determine the precise position of the probe, is currently underway.

**Saxitoxin Derivatives.** Saxitoxin derivatization is proceeding slowly, with our only attempts being the decarbamylation of STX thusfar. This intermediate (see Figure 19) is necessary for the construction of all other derivatives. We are attempting to conserve precious STX starting material, and are working in 1 mg quantities. With the availability of more STX in the near future, we shall increase volume and reaction quantities slightly. We anticipate the decarbamoyl derivative to be optimized in 3 months.

With respect to saxitoxin synthesis, we are at step 5 (Figure 21) in the overall synthesis but have had difficulty in construction of the mesylate derivative. Low yields in step three of the synthesis prevent massive scale-up to produce the amount of material we desire for further work. It is our intent to try some minor protective modifications of cyano functionalities to increase yields. The Kishi synthesis in our hands produces less than the 75% yield he reports [19]. Once we have overcome this difficulty, synthesis of the entire molecule should conclude within 3 months. This should yield racemic STX, which shall be separated on a chiral column to yield the two enantiomers of STX. Both materials should be of interest in further work.

**Tetrodotoxin Derivatives.** Trityl, dimethoxytrityl, trimethoxytrityl, and *t*-butyldimethylsilyl tetrodotoxin have been synthesized (Figure 13). Primary alcohol protected TTX has been benzylated (Figure 15a) and the primary alcohol deprotected (Figure 15b). The deprotected material has been sent off for elemental analysis to confirm identity. This secondary-protected, primary-deprotected material is necessary for the synthesis of all the other derivatives except one affinity column. The same protocols will be used with this alcohol function as will be used for decarbamoyl saxitoxin (also a primary alcohol). Anhydroepitetrodotoxin (Figure 17) has been synthesized and has been coupled to aminohexyl Sepharose (Figure 17 b) to produce aminohexyltetrodotoxinamide AH Sepharose. The advantage of this toxin affinity column is that both the guanidinium function and the primary alcohol function are free to interact with receptors. This affinity column binds solubilized synaptosomes, can be extensively washed to clean up the preparation, and can then be eluted with high salt to detect a high molecular weight protein which can be identified on SDS-PAGE as being near the size range for  $\alpha$ -subunit of sodium channel. The stoichiometry of toxin covalent modification to bind to the matrix, and the subsequent binding of protein to the column is currently under evaluation.

**Brevetoxin Derivatives.** Tritiated brevetoxin is available. Brevetoxin-*p*-azidobenzoic acid (Figure 10) at 10 Ci/mmol and unlabeled have both been synthesized. Ring tritiated *p*-azidobenzoic acid-brevetoxin is under current evaluation. Brevetoxin-3-*p*-azidophenyl-2-*p*-hydroxyphenyl propionic acid photoaffinity probe has been synthesized. Brevetoxin aminohexyl Sepharose columns have been synthesized with a specific toxin capacity of 4-6  $\mu$ mol/mL resin. Additional derivatives are under development.

**Photoaffinity Probes.** The unmodified probes illustrated in Figures 4-7 and Figure 9 have been synthesized. Tritiated (60 Ci/mmol) *p*-azidobenzoic acid is being synthesized (radioactive Figure 9).

## CONCLUSIONS

Our work thus far on this contract has succeeded in identifying the domain within which the brevetoxin photoaffinity probe binds. We have succeeded in synthesizing each of the toxin derivatives necessary to complete this effort, and have gained considerable expertise in micro-organic chemistry. We anticipate that our continued effort on the contract will result in as many different derivatives for saxitoxin, tetrodotoxin, and veratridine as we have produced for brevetoxin. We expect that we shall be able to define the specific binding sites on the VSSC for the binding of these toxins using the derivatives produced. Overall, we expect to be able to define the spatial topographic relationship between the sites with the information we continue to collect. Specifically, we feel that our effort will be directed in the following ways:

(1) **Photoaffinity Reagents.** These have been characterized and shall be utilized for each of the classes of toxin described when the appropriate toxin derivative is available. The anticipated availability of tritiated *p*-azidobenzoic acid allows for the construction of very hot toxin probes without the necessity of tritiated toxin. Recommended further effort: continue coupling efforts;

(2) **Affinity Columns.** The brevetoxin affinity column has been synthesized and binds specific antibrevetoxin (not described) antibody with high affinity. The tetrodotoxin affinity column binds proteins from solubilized synaptosomes. Recommended further effort: Brevetoxin affinity column ready for shipment as a Deliverable. Continue characterization of tetrodotoxin affinity column including stoichiometry of covalent toxin binding to matrix, and characterization of the affinity purification of proteins from synaptosomes;

- (3) Tetrodotoxin Modifications. Continue attempts at producing primary alcohol de-protected and secondary alcohol-protected tetrodotoxin for construction of the rest of the TTX derivatives. Recommended further effort: Secure 50 mg additional TTX from commercial suppliers to continue the effort. Focus effort first on production of non-exchangeable tritium-labeled TTX (Figure 16);
- (4) Saxitoxin Derivatives. Continue characterization of decarbamoyl saxitoxin and optimize derivative for further work. Recommended further effort: Proceed with oxidation of primary alcohol in decarbamoyl STX first in preparation for re-reduction using borotritide to produce non-exchangeable tritiated STX. Using deprotected primary alcohol benzylated saxitoxin, begin synthesis of each of the additional derivatives;
- (5) Saxitoxin Synthesis. We have gotten through 5 steps of our saxitoxin synthesis; and three of them with very high yields. We anticipate optimization of step 3-5 to allow us to proceed to completion. Recommended further effort: Use cyano-protecting agents to increase yields of 3-5. Repeat steps 1-3 to obtain more reaction intermediate for later steps. Explore remaining steps to completion to produce racemic saxitoxin. Separate materials obtained by chiral HPLC and supply both as deliverables;
- (6) Brevetoxin Binding Site. We expect this work to be complete by year's end. We have isolated the brevetoxin photoprobe binding site to Domain IV of the VSSC  $\alpha$ -subunit, and have shown it interacts with the extracellular polypeptide between S5 and S6 of that domain. Recommended further work: repeat photoprobe experiments using the 60 Ci/mole brevetoxin photoaffinity probe once synthesized. Repeat immunoprecipitation experiments using anti SP antibodies. Trypsinize the domain and separate peptides generated by HPLC. Isolate and characterize the tritiated peptide fragment generated. Begin sequencing of the tritiated peptide to define the exact amino acid of brevetoxin interaction;
- (7) Brevetoxin Derivatives. Columns have been completed. Radioactive (10 Ci/mole) brevetoxin has been synthesized. Photoprobes have been synthesized. Recommended further effort: Begin enzyme-synthesized high specific activity brevetoxin work. Explore high specific activity NADH tritium incorporation. Begin culturing *P. brevis* in presence of  $^{14}\text{C}$  bicarbonate to produce carbon-labeled brevetoxin;
- (8) Binding Sites 1, 2, and 5 Comparison. With the availability of the reagents for sites 1 and 2, we shall begin comparison with site 5. Based on our excellent progress with Site 5, we expect to begin this phase of the work in 6 months. Recommended further effort: begin site 1 using the TTX affinity column and compare with site 5 SDS-PAGE. Attempt  $^{32}\text{P}$  labeling of the TTX affinity column material to assess  $\alpha$ -subunit potential. Begin derivatization of site 2 ligand veratridine. Insufficient batrachotoxin is available for the effort. Compare the photoaffinity bound tritium from each site specific ligand by immunoprecipitation and trypsinization as worked out for the brevetoxins.

## REFERENCES

- [1] Wu, C.H., and Narahashi, T. (1987) *Annu. Rev. Pharmacol. Toxicol.* 28, 141-161.
- [2] Strichartz, G., Rando, T., and Wang, G.K. (1987) *Annu. Rev. Neurosci.* 10, 237-267.
- [3] Ellis, S. (1985) *Toxicon* 23, 469-472 [introduction for a collection of papers on brevetoxins contained in the same issue].
- [4] Catterall, W.A., and Risk, M.A. (1981) *Molec. Pharmacol.* 19, 345-348.
- [5] Poli, M.A., Mende, T.J., and Baden, D.G. (1986) *Molec. Pharmacol.* 30, 129-135.
- [6] Sharkey, R.G., Jover, E., Jouraud, F., Baden, D.G., and Catterall, W.A. (1987) *Molec. Pharmacol.* 31, 273-278.
- [7] Catterall, W.A., and Gainer, M. (1985) *Toxicon* 23, 497-504.
- [8] Lombet, A., Bidard, J.N., and Lazdunski, M. (1987) *FEBS Lett.* 219, 355-359.
- [9] Frelin, C., Durand-Clement, M., Bidard, J.N., and Lazdunski, M. (1990) pp. 192-201. In *Marine Toxins: Origin, Structure, and Molecular Pharmacology* (S. Hall and G. Strichartz, Eds.) American Chemical Society Symposium Series Vol 418, Washington, D.C.
- [10] Moczydlowski, E., Olivera, B., Gray, W.R., and Strichartz, G.R. (1986) *Proc. Natl. Acad. Sci. USA* 83, 5321-5325.
- [11] Bidard, J.N., Vijverberg, H.P.M., Frelin, C., Chunque, E., Legrand, A.M., Bagnis, R., and Lazdunski, M. (1984) *J. Biol. Chem.* 259, 8353-8357.
- [12] Gusovsky, F., Rossignol, D.P., McNeal, E.T., and Daly, J.W. (1988) *Proc. Natl. Acad. Sci. USA* 85, 1272-1276.
- [13] Baden, D.G. (1989) *FASEB J.* 3, 1807-1817.
- [14] Catterall, W.A. (1985) pp. 103-122. In *Neurotransmitter Receptor Binding* (Yamamura, H., Enna, S., and M. Kuhar, Eds.) Raven Press, N.Y.
- [15] Catterall, W.A. (1989) *ICSU Short Reports* 9, 14-15.
- [16] Messner, D.J., Feller, D.J., Scheuer, T., and Catterall, W.A. (1986) *J. Biol. Chem.* 261, 14882-14890.
- [17] Noda, M., Ikeda, T., Kayano, T., Suzuki, H., Takeshima, H., Kurasaki, M., Takahashi, H., and Numa, S. (1986) *Nature* 320, 188-192.
- [18] Tanabe, T., Takeshima, H., Mikami, A., Flockerzi, V., Takahashi, H., Kangawa, K., Kojima, M., Matsuo, H., Hirose, T., and Numa, S. (1987) *Nature* 328, 313-318.
- [19] Kishi, Y. (1980) *Heterocycles* 14, 1477.
- [20] Koehn, F.E., Ghazarossian, E., Schantz, E.J., Schnoes, H.K., and Strong, F.M. (1981) *Bioorganic Chemistry* 10, 412-428.
- [21] Laemmli, U.K. (1970) *Nature* 227, 680-685.
- [22] Blattler, D.P., Garner, F., VanSlyke, K., and Bradley, A. (1972) *J. Chromatogr.* 64, 147.



- [23] Weber, K., and Osburn, M. (1969) *J. Biol. Chem.* 224, 4406-4412.
- [24] Hartsborne, R.P., Coppersmith, J., and Catterall, W.A. (1980). *J. Biol. Chem.* 225, 10572.
- [25] Schmidt, J., Rossie, S., and Catterall, W.A. (1985) *PNAS* 82, 4847-4851.

**SUPPLEMENTARY**

**INFORMATION**

## ERRATA

Tris-HCl (pH 8) was added and the mixture was incubated at 100°C for 1 min. After cooling to 4°C, this solution was loaded on the column.

(6) Neuraminidase treatment. Two mL aliquots of the putative  $\alpha$ -subunit were recovered from the 2-mercaptoethanol treatment and incubated with 0.1 unit of neuraminidase at 37°C for 5 hr. One-half mL aliquots of each digest were added to the Sephacryl column.

(7) Endoglycosidase F. One-half mL aliquots of the putative  $\alpha$ -subunit were recovered from neuraminidase-treated column eluents. One-half mL of buffer containing 0.1% SDS, 2% Nonidet P-40, 2% 2-mercaptoethanol, and 100 mM EDTA, pH 6.1 were added prior to the addition of 1 U endoglycosidase F to each vial. The solution was incubated at 37°C for 16 hr and digestion was terminated by adjusting the SDS concentration to 2% and boiling for 2 min. One mL of the final solution was loaded on the Sephacryl column.

(8) Bio-Bead SM-2 purification. The eluent from the Sephacryl S-300 column was incubated with 1/5 volume of Bio-Beads SM2 (Bio-Rad) overnight at 4°C with agitation. After centrifugation at 15,000  $\times$  g for 3 min, both pellet and supernatant solution were assayed for radioactivity.

(9) Bligh and Dyer extraction. To 0.4 mL of pooled protein fractions from the Sephacryl S-300 column, 1 mL methanol and 0.5 mL chloroform were added and the mixture shaken to form an azeotrope. Distilled water (0.4 mL) and 0.4 mL chloroform were added and layers were allowed to separate; and were assayed for radioactivity.

(10) Ion exchange and wheat germ allutinin-Sepharose chromatography. Methods used were similar to those published by Hartshorne and Catterall [referenced in 14]. Modifications were made in elution buffers used with both type of column. The [<sup>3</sup>H]breve toxin-photolabeled sodium channel (NaTPHO) was eluted from DEAE Sephadex A-25 with 1 M KCl and from the WGA-Sepharose column with 0.3 M N-acetylglucosamine (NAG).

(11) Trypsinization of photoaffinity-bound sodium channel. NaTPHO taken through the WGA-Sepharose purification step was dialyzed against distilled water, and then lyophilized. The NaTPHO was resuspended in a volume of Buffer S (10 mM Tris-HCl, pH 7.4, 150 mM NaCl, 1 mM EDTA, 0.1% Triton X-100) which resulted in approximately 2000 DPM per 25  $\mu$ L. TPCK-trypsin (Worthington) was added to give a final concentration of 10 mg/mL. The solution was incubated for the designated time (results section) and the reaction was stopped by adding an equal volume of SDS sample buffer containing 2-mercaptoethanol. Samples were incubated at 100°C for 2 min, allowed to cool to room temperature, and subjected to SDS-PAGE and assessment.

(12) Immunoprecipitation. WGA-Sepharose purified NaTPHO was resuspended in Buffer S to give a final activity of 1000 DPM/50 mL. One tenth final volume of TPCK-trypsin or Buffer S was added and the sample digested for the times indicated. After addition of 0.1% SDS, the sample was incubated at 100°C for 3 min, cooled by swirling on ice. Trypsin inhibitor (Sigma) was added to a final concentration of 50  $\mu$ g/mL and incubated for 5-10 min. The following series of effectors were then added to give the indicated final concentrations: 1% Triton X-100, 150 mM NaCl, 0.5 mg/mL BSA. The appropriate antisodium channel antibody was added to give a final concentration of 1.2 mg/mL. The reaction mixture was incubated with rotation at 4°C overnight. Fifteen mg Protein A-Sepharose, swollen for 1 hr in TBS buffer (0.5 mg/mL BSA, 20 mM Tris, pH 7.4, 150 mM NaCl, 1% Triton X-100) was added and incubated for 45 min. The samples were centrifuged for 15 sec in a microfuge, the supernatant solutions were discarded, and the pellets resuspended in 1 mL TBS. This was repeated twice more. The resulting pellet was assayed for radioactivity.

(13) Antisodium channel antibodies. These were supplied by Dr. W.A. Catterall as part of a collaborative study.

(14) Radioimmunoassay. Varying concentrations of antibody were added to 0.1 M glycine, pH 7.4 and incubated with 5 pmole <sup>32</sup>P-sodium channel in NET buffer (75 mM NaCl, 2.5 mM EDTA, 25 mM Tris, pH 7.4, 0.1% Triton X-100, 50 mM NaH<sub>2</sub>PO<sub>4</sub>, 20 mM KF). This mixture was incubated for 4-16 hr at 4°C with rotation. Five mg Protein A-Sepharose, swollen 1 hr in NET buffer, was added and the solution incubated for 45 min on ice. The sample was centrifuged at 4°C for 15 sec and the supernatant was discarded. One mL NET buffer was added, the sample resuspended and centrifuged as before. This was repeated twice more.

(15) Phosphorylation of WGA-purified sodium channel. This method was described by Schmidt *et al.* [25]. Briefly, 500 pmole sodium channel purified through the step of WGA-Sepharose was added to a solution of 100  $\mu$ M ATP, 10 mM MgCl<sub>2</sub>, 0.05% Triton X-100, 0.1  $\mu$ g/pmol cAMP-dependent protein kinase, 0.25  $\mu$ Ci/pmol <sup>32</sup>P ATP and incubated for 60 min on ice. The reaction was stopped by the addition of EDTA at 20 mM final concentration. The mixture was then centrifuged through several G-50 columns pre-equilibrated with NET buffer. The column eluent was assayed for radioactivity.